BSA SERVICES

FINAL REPORT

Contract No. NAS 9-18493

covering period
10/24/90 - 6/31/91

Three tasks were defined in the SOW; (1) Spectral Fitting of Current Data, (2) Shock Layer Modeling Using DSMC Code, and (3) Production of Nitrogen Oxides and Excited Nitrogen in Flow Fields. All three tasks were carried forward satisfactorily over the given time period with some alteration from the initial set of subtasks. Some changes due to the nature of the research, approved by the technical monitor, provided results beyond the scope of the original proposal. An abstract was completed, resulting from efforts on task 3, and the full paper, scheduled for presentation at an AIAA meeting in January, is near its final form.

Task 1 - Spectral Fitting of Current Data (320/110 hrs)

Proposed. It was proposed that analysis of N_2 emission from 8.72 MJ/kg shock layer be made at 2.54, 1.91, and 1.27 cm positions and that vibrational state distributions, temperatures, and relative electronic state populations be obtained from data sets. It was further proposed to review other recorded arc-jet N_2 and air spectral data and to study NO emission characteristics characteristics in data. Spectra of selected data sets was to be analyzed for an abstract and technical report or journal paper.

Accomplished. It was possible to adjust analysis techniques such that relative populations of two electronic states, the $B^3\Sigma$ state of the neutral molecule and the $A^2\Pi$ state of the molecular nitrogen ion could be determined for four positions within the 8.72 MJ/kg shock layer. Results show a change in population distributions and overall relative population between the two electronic states as one moves from the front of the shock to the boundary layer. Also, preliminary data has been obtained on relative populations between the first two excited electronic states of the ion , $A^2\Pi$ and $B^2\Sigma$. Such population ratios, an example of which is given in Appendix A, will provide information on electronic state distributions or electronic temperatures. Use was made of the PSI code over a range from 350 nm to 800 nm was made for these results.

Evaluation of accuracy in the overall analysis was thought necessary and additional time has been used in evaluating errors. Since vibrational temperature analysis techniques require rotational temperature input, rotational temperature was again investigated using a different method of evaluation. The method was based on that used by Leger, et al. in a nitrogen plasma jet

study reported from France in 1990. Rotational temperature analysis is made using the NEQAIR code and new results show differences on the order of 300 K from previous measurements. This represents differences of only 4-8%, about equivalent to the accuracy of analysis. Additional information may be found in Appendix B.

Other recorded arc-jet N_2 and air spectral data were reviewed and a technical report covering this data initiated. Part of that information is displayed in Appendix C. There are six air data sets, all taken near the front of the shock. Of the three N_2 data sets, two sets were taken at the improved spatial resolution and only only one of those, that from which much of the previous analysis has come, covers four points within the shock layer.

Recommended. For improvement in the accuracy of analysis where long wavelength spans are necessary a change in the NEQAIR code from 20,000 to 40,000 points is recommended. But Park's updated code is likely set at 40,000 and likely will run on the cray without the modification of our current code. The $A^2\Pi$ state it should be added to that code. Excitation as well as radiation data will be required. For the type of measurements desired the PSI code requires improved accuracy in radiation data for states above v' = 12.

Task 2 - Shock Layer Modeling Using DSMC Code (173/60 hrs)

Proposed. A review of operational procedures of the then current JSC DSMC code was proposed. Information on other appropriate codes and modifications, including ionization, were to be made, and a determination of the applicability of codes reviewed to task requirement and comparison of computational capabilities and input variables was proposed.

Accomplished. Two versions of the JSC DSMC code were found and their computational procedures were reviewed. An additional variation of the Bird DSMC code format was subsequently obtained from Sandia. The JSC code operated on the VAX had been modified for time sequence file output for particular plot considerations. Concentration was eventually made on the other JSC code operation from the cray. Studies were first made using simple boundary parameters for a spherical body as test article.

New region and cell boundary parameters were identified by Scott for a flow investigation of a mass spectrometer probe system. The configuration is given in Appendix D. It was basically shown that the computational procedures could be used for this application, a relatively complex configuration, but some detail changes and additions to the code, such as wall catalysis, are being reviewed in order to make the results more useful. A plot routine placed on the Iris workstation was determined most ideal for the type of data reduction required, but no significant plots were obtained for inclusion in this report.

Recommended. Acquisition and modification of a code which includes ionization and radiation from Langley or a developmental effort is recommended.

Task 3 - Production of Nitrogen Oxides and Excited Nitrogen in Flow Fields (976 hrs)

Proposed. It was proposed that a review be made of computational procedures used in CFD codes of Li and other codes on JSC computers and that the literature related to task objectives be reviewed. Analysis of problems associated with integration of specific chemical kinetics applicable to task into CFD codes was to be made.

Accomplished. Computational procedures and literature related to the task objectives were reviewed. Results of this initial task led to a greater emphasis being placed in the analysis upon computation of basic model parameters required for CFD input, the excitation and relaxation of the nitrogen molecule.

The diffusion equation, derived from the master equation for the electron-impact vibrational relaxation based on the diffusion approximation, was numerically solved for evaluation of time variations of vibrational number densities of each energy level and of the total vibrational energy. Subsequently, an approximate rate equation and a corresponding electron-impact vibrational relaxation time from the excited states was derived, compatible with the system of flow conservation equations. This represented the first such derivation considering multiple-quantum transitions from excited states to higher/lower states for the electronic ground state of the nitrogen molecule.

The empirical curve-fit formulae for the improved relaxation time, which will be convenient for actual CFD flow calculations, were obtained using two quadratics in the logarithm of the electron temperature. The solution of the master equation for the e-V process shows a non-Boltzmann population distribution at the earlier stage of relaxation, which in turn suppresses the equilibration process. These results will be presented at the AIAA 30th Aerospace Sciences Meeting at Reno in January, 1992, as a paper titled Electron-Impact Vibrational Relaxation in High-Temperature Nitrogen. The abstract is included as Appendix E.

Recommended. Further development of the approximate rate equation, which accounts for the non-Boltzmann nature of the population distribution is recommended. Analysis should be made for the rotational excitation process and the electronic excitation distribution of N_2 molecules at very high temperatures.

Preliminary Population Distributions at 3.18 cm

v'	N2(A)	N2+(A)	N2+(B)
0			8.10E+09
1			5.27E+09
2	1.74E+12	2.47E+12	3.06E+09
3	0.00E+00	2.72E+12	2.38E+09
4	1.44E+12	0.00E+00	2.07E+11
5	0.00E+00	1.25E+12	
6	9.69E+11	0.00E+00	
7	7.81E+11	0.00E+00	
8	2.12E+11	0.00E+00	
9	3.61E+11	0.00E+00	
10	0.00E+00	4.99E+11	
11	3.56E+11		
12	8.35E+11		

Preliminary Population Distributions at 2.54 cm

v'	N2(A)	N2+(A)	N2+(B)
0			2.66E+10
1			1.63E+10
2	7.49E+12	6.67E+12	8.30E+09
3	0.00E+00	6.88E+12	6.07E+09
4	3.81E+11	0.00E+00	5.31E+09
5	0.00E+00	3.62E+12	
6	2.98E+11	2.33E+12	
7	9.22E+11	1.21E+12	
8	0.00E+00	5.58E+10	
9	0.00E+00	1.16E+12	
10	1.36E+12	0.00E+00	
11	8.65E+11		
12	2.08E+12		

The population data shows first zeros populations for some vibrational levels indicating problems and unreliability of the numbers, those from the N_2 and N_2^+ (A)-states particularly. The A-states of neutral molecule and ion produce radiation within the same wavelength range, so the problems with the fit are understood, requiring refinement in the process and additional vibrational data. The nonzero numbers, however, although inaccurate, represent reasonable relative populations for the vibrational states.

A rough estimation of relative populations of the electronic states may be made, for example, by looking at the vibrational state populations for v' = 2. That would yield

$N_2(A)/N_2^+(A) = 0.7$ at 3.18 cm
$N_2(A)/N_2^+(A) = 1.1$ at 2.54 cm

$N_2^+(A)/N_2^+(B) = 807$ at 3.18 cm
$N_2^+(A)/N_2^+(B) = 803$ at 2.54 cm

The latter two ratios would indicate little change in the electronic temperature of N_2^+ between the two positions, but the first two indicate an increase in the relative population of the neutral molecule.

Additional analysis as well as greater accuracy is necessary before definitive arguments will be made. The additional data and analysis will be presented in the completed paper.

APPENDIX B

One problem in determining rotational temperature is the overlaping of the P and R branches in the first negative system of the ion where the measurement is usually made. In such cases the overlapped lines define global lines from which it is possible to define a rotational temperature. Following the method used by Leger, the line intensity distribution as a function of temperature, t, would be

$$\varepsilon(\lambda,t) = \varepsilon_p(\lambda) + \varepsilon_r(\lambda)$$

a sum of integrated intensities of rotational lines of the P and R branches falling within an unresolved wavelength range with a peak at wavelength λ. With much of the bandhead unresolved and consisting primarily of lines from the P branch, a bandhead intensity is defined by

$$\varepsilon_{head} = \sum_{K=1}^{24} \varepsilon_p(K,t)$$

where K is the total angular momentum quantum number apart from spin. Using the ratio,

$$I(t) = \frac{\varepsilon(\lambda,t)}{\varepsilon_{head}}$$

for both computed, in our case by NEQAIR, and experimental spectra, a function

$$E(t) = \frac{1}{N}\left[\sum_{i=1}^{N} \left(I_i\,(exp) - I\,(cal)\right)^2\right]^{\frac{1}{2}}$$

using a square of differences is defined. Here N is the number of global lines, six in our case. Executing the least squares technique, with NEQAIR providing the calcuated intensities as a function of equilibrium temperature, the measured rotational temperature is that which minimizes E(t).

Previous measurements utilized a different spectral matching and ratio technique. Those measurements have been repeated using the above technique and a comparison between results is given below.

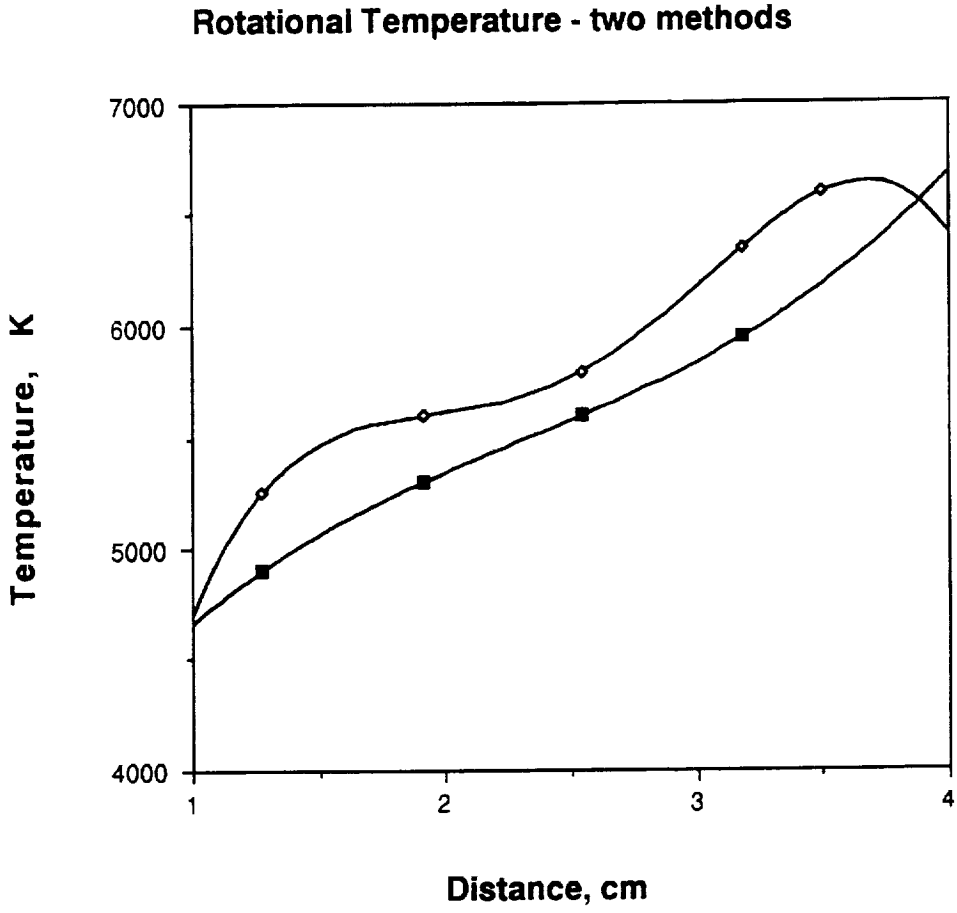

The lower line in the graph represents the older measurements. Subsequent analysis of the new measurements show a sensitivity to careful matching of computed spectral characteristics to experimental spectra.

A view of the spectral lines, as given in the series of data which follow, shows that the peak intensities of the rotational lines do not follow a normat temperature distribution. Consequently one cannot guess at a temperature by looking at the distribution. Although it appears to be a fluctuation phenomena which causes some error, temperatures can be inferred.

run with nn2 min at 6350

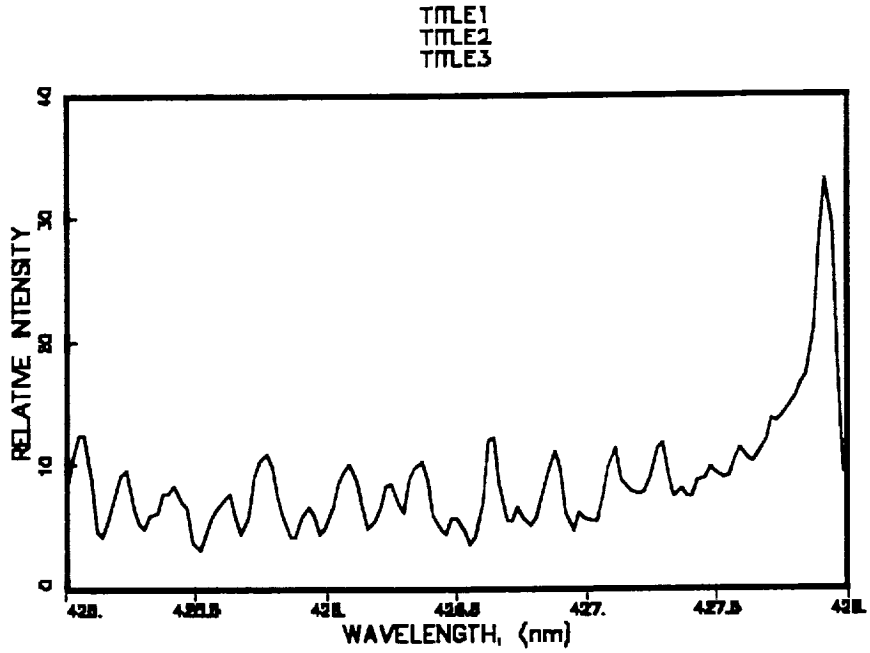

run with nn3 min at 5800

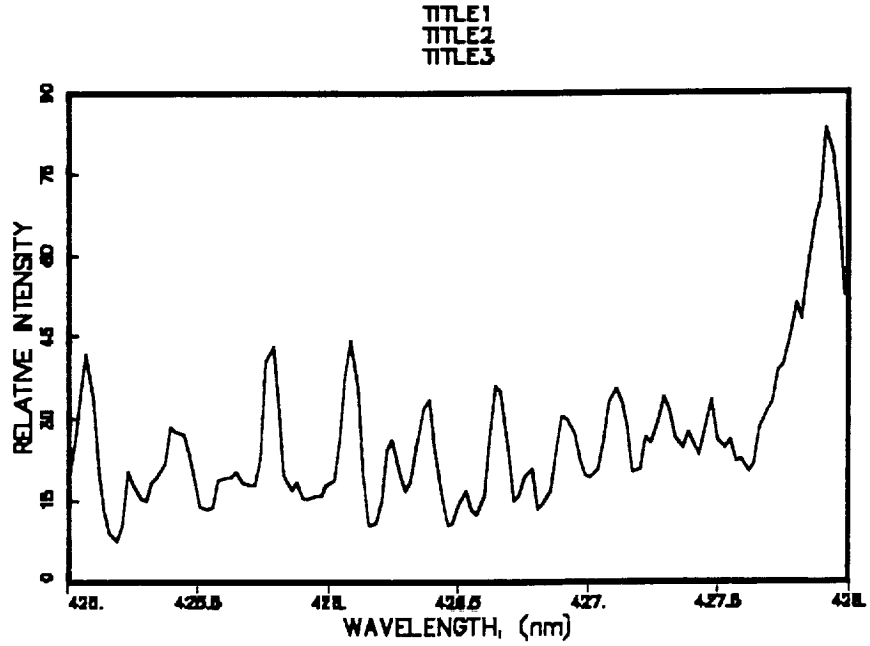

run with nn4 min at 5600

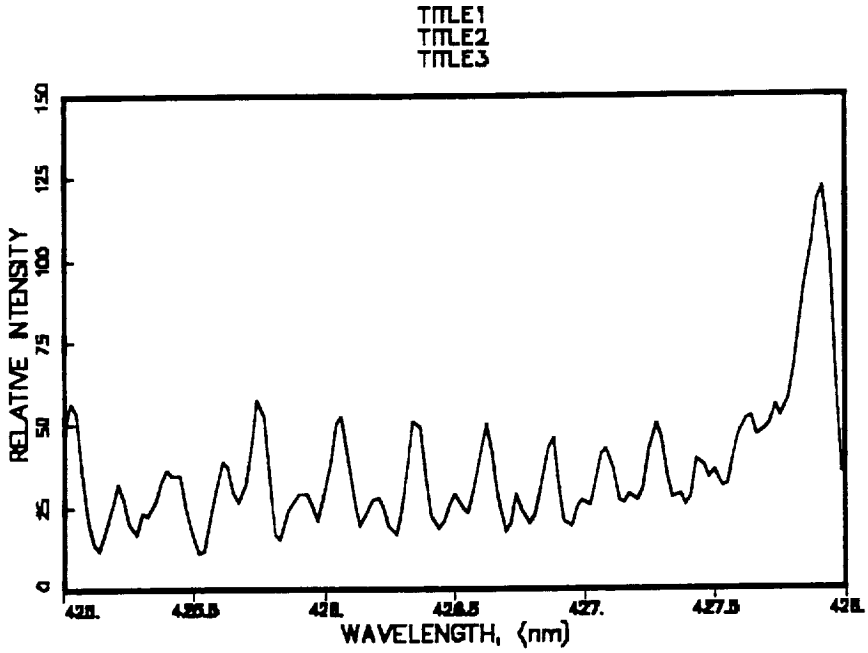

nn5 min 5250

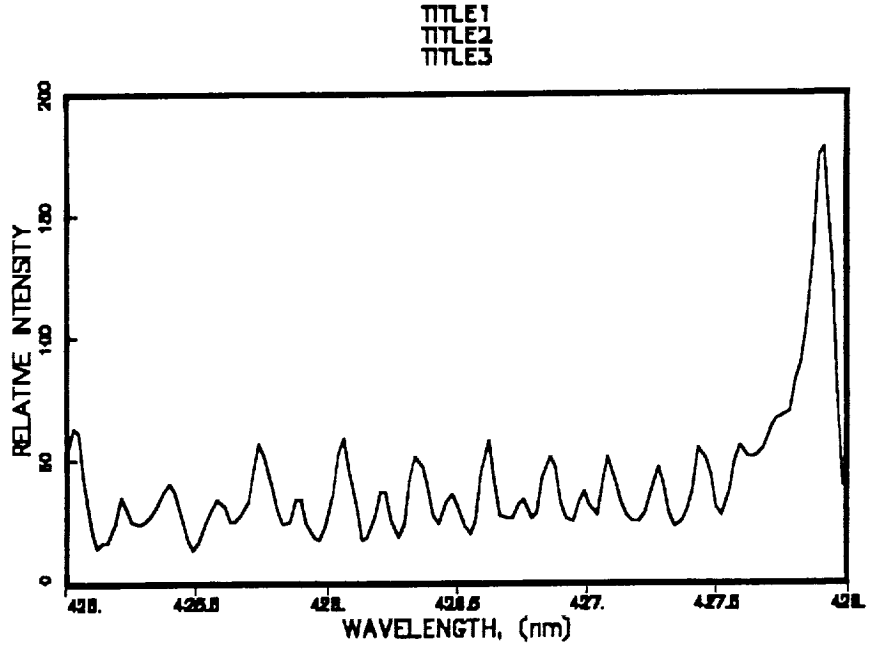

APPENDIX C

ARC JET DATA SETS

LABEL	pixels	GAS	CURRENT amp	FLOW RATE lbs/s	ENTHALPY J/kg	DISTANCE cm	GRATING
C	7412	air	1100	0.08			600
D	7408	air	600	0.04		3.5	600
E	7903	air	800	0.08		3.5	600
F	8333	air	800	0.08		3.5	600
I	8333	air	800	0.08		3.5	600
J	8333	N2	500	0.08		3.5	600
K	8333	air	1000	0.12		3.5	600
L	8332	N2	600	0.12		3.5	600
LL	8333	N2	600	0.12		2.5	600
L2	3741	N2	600	0.12		3.5	1800
LL2	3741	N2	600	0.12		2.5	1800
N2	9620	N2	600	0.12		3.18	600
N3	9192	N2	600	0.12		2.54	600
N4	9192	N2	600	0.12		1.91	600
N5	9192	N2	600	0.12		1.27	600
NN2	3741	N2	600	0.12		3.18	1800
NN3	3741	N2	600	0.12		2.54	1800
NN4	3741	N2	600	0.12		1.91	1800
NN5	3741	N2	600	0.12		1.27	1800

The most significant analysis has been made using the N- series, where data was collected from four points within an N2 shock layer.

The following spectra were taken at a low flow rate, 0.04 lbs/s, with an arc current of 600 A. These spectra correspond to that labeled D above.

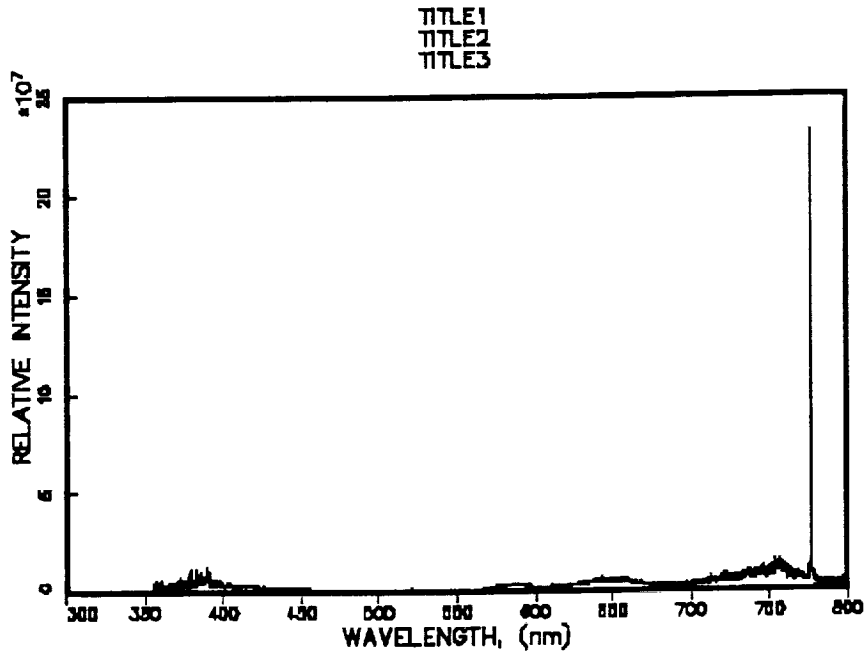

D

The spectrum between 300 and 800 nm shows a single strong atomic line at 760 nm. A closer look at the spectrum below 700 nm is shown below.

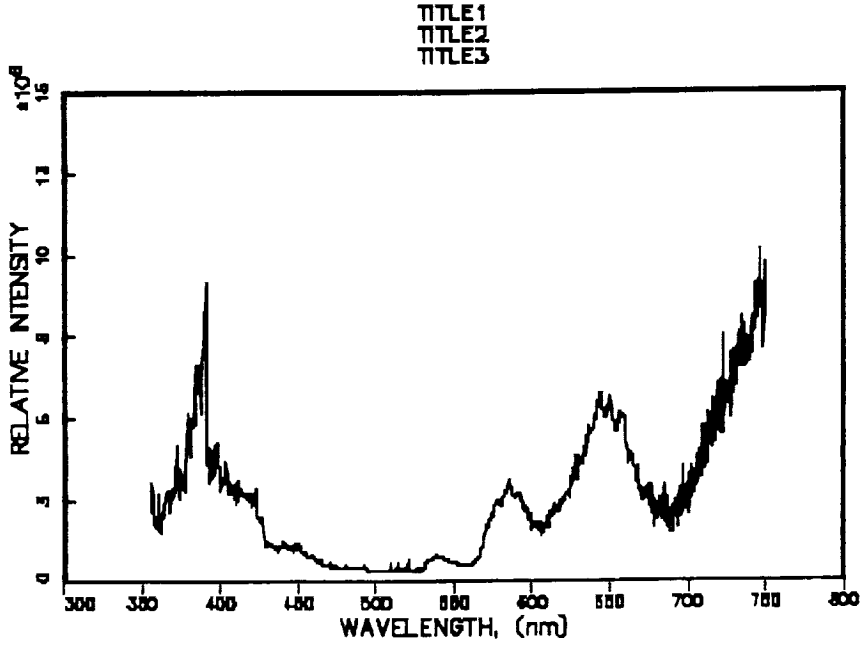

While the first positive N_2 bands appear clear for analysis, the first negative N_2^+ bands are obscured by NO radiation. To analize the N_2 radiation bands for an accurate vibrational temperature or population distribution, a rotational temperature is needed (estimates can be made, however, through spectral matching in the analysis of vibration). Although analysis of the shortwavelength radiation, shown in greater detail in the following three spectral plots, appears exceptionally difficult, improved tools may allow significant information to be obtained.

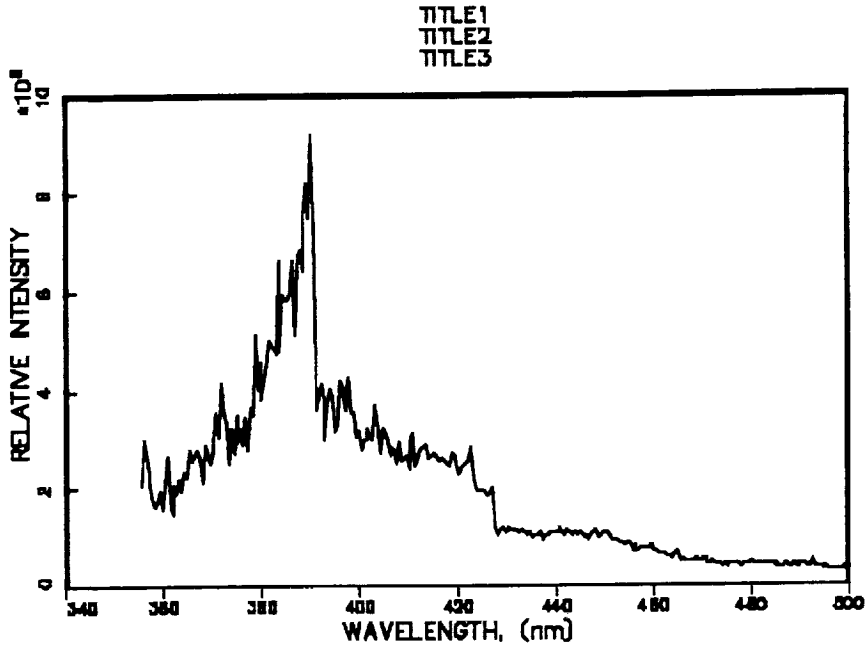

D

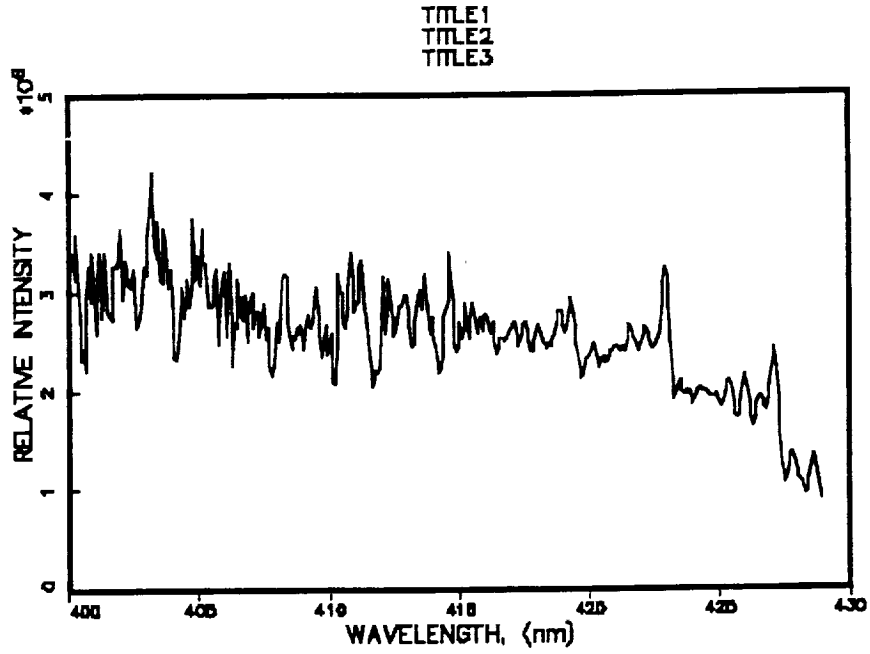

D

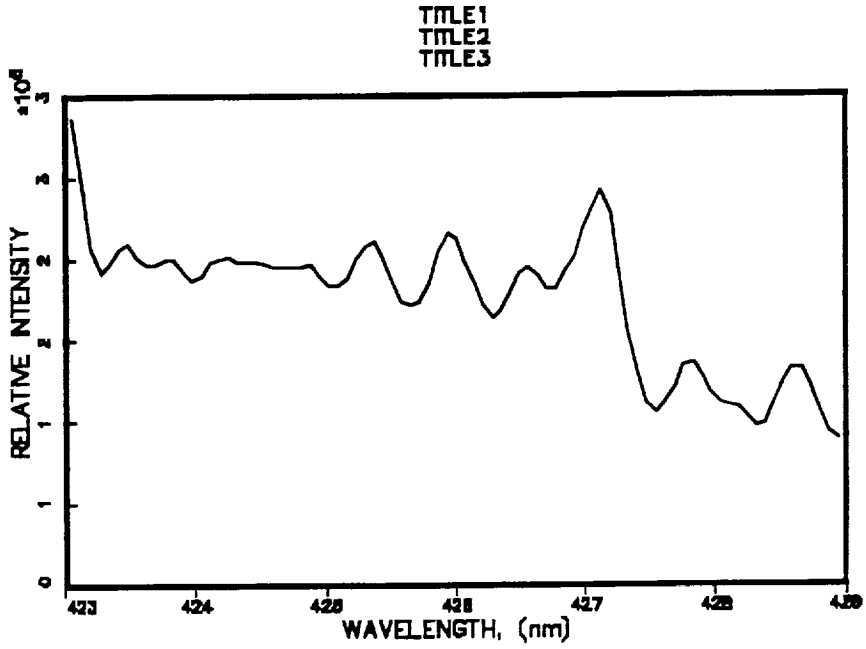

D

Radiation overlaping the N2+ bandheads in the spectra above can be seen.

The bandheads at 800 A, 0.08 lb/s, labeled E, appears clearer as the 2nd positive system of N_2 replaces the NO radiation.

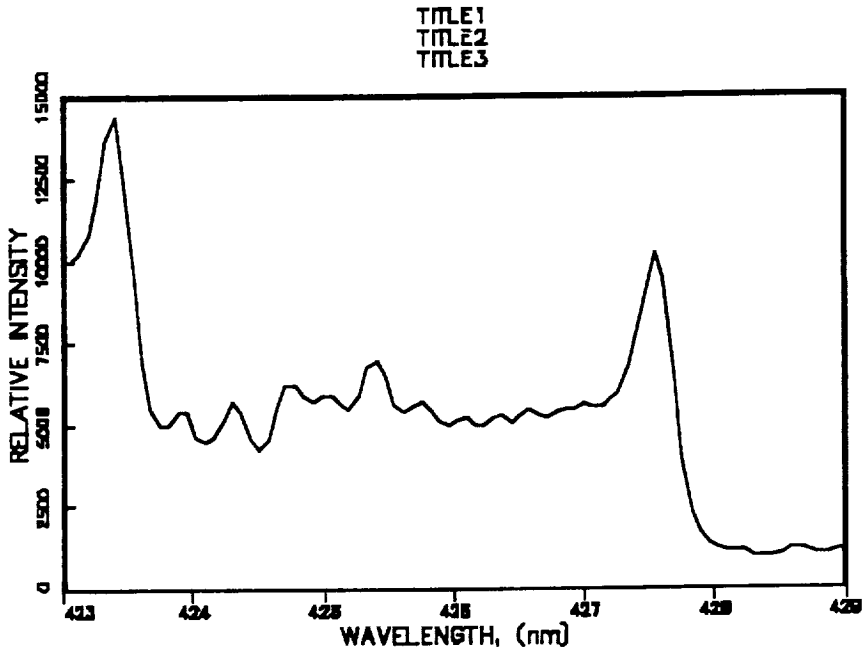

E

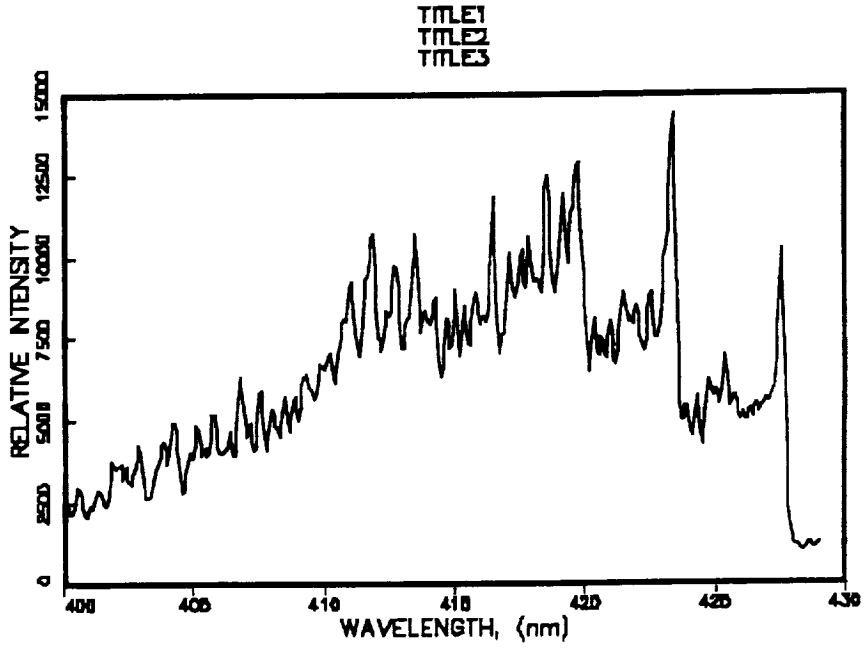

E

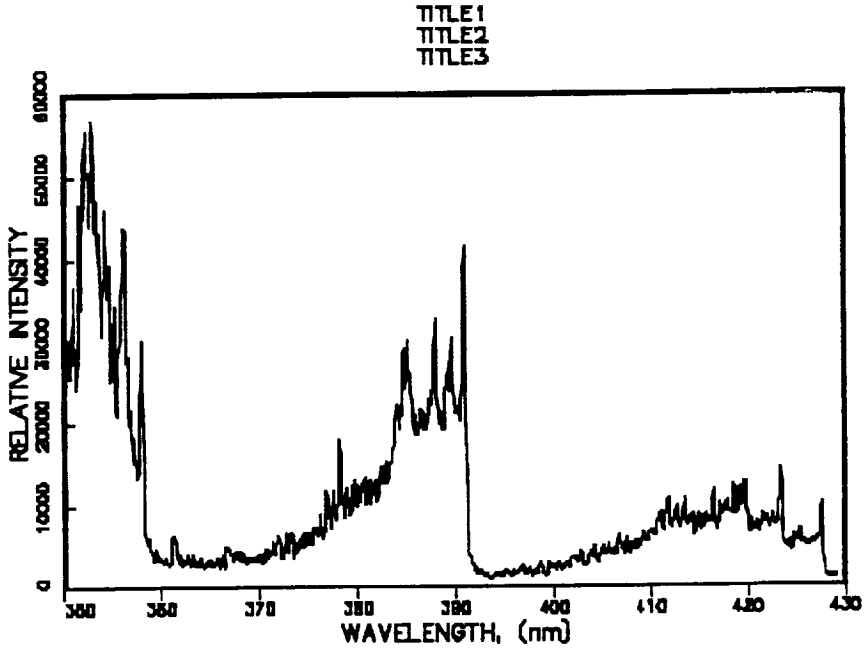
TITLE1
TITLE2
TITLE3
RELATIVE INTENSITY
WAVELENGTH, (nm)

E

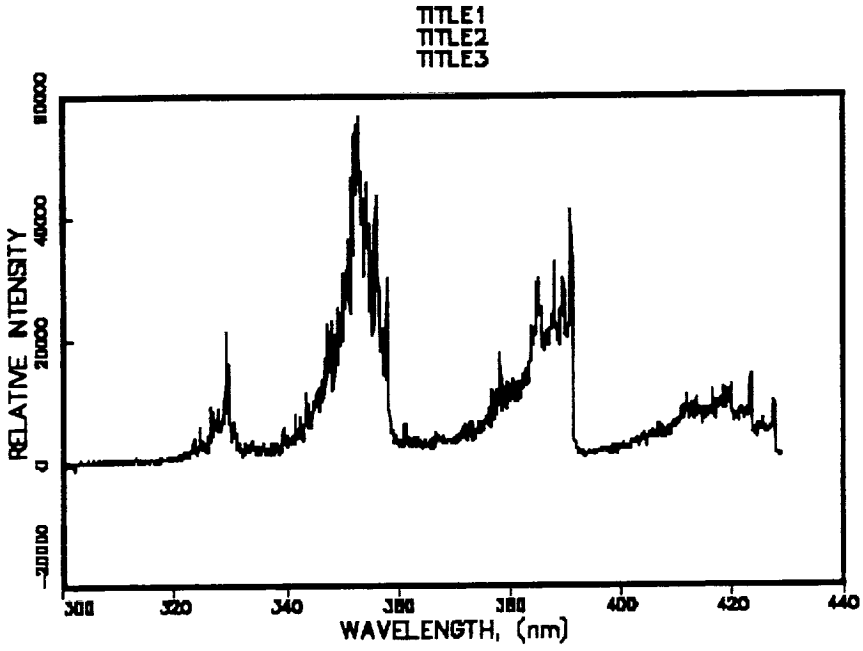
TITLE1
TITLE2
TITLE3
RELATIVE INTENSITY
WAVELENGTH, (nm)

E

Differences can be seen in the spectra labeled C with current increased to 1100 A at 0.08 lb/s.

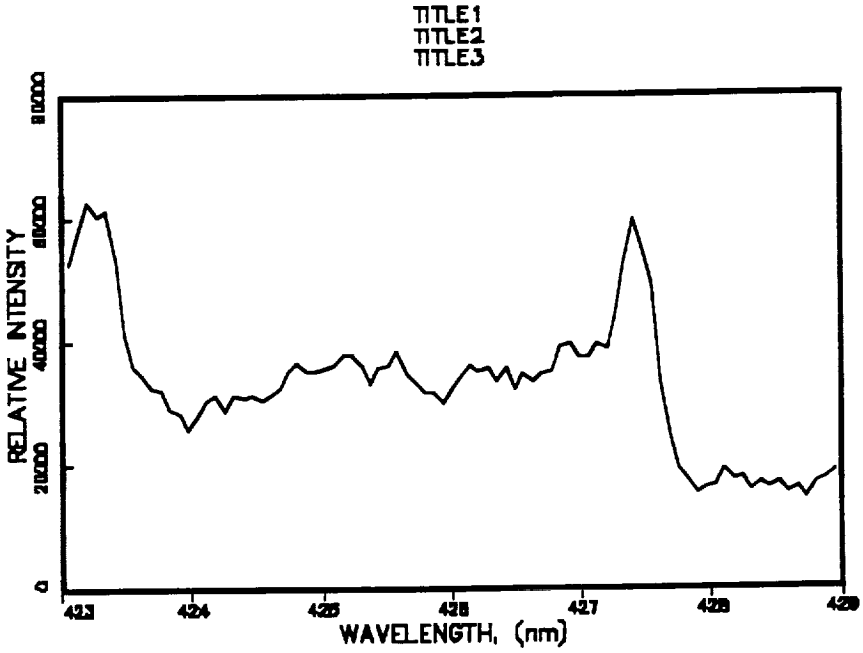

C

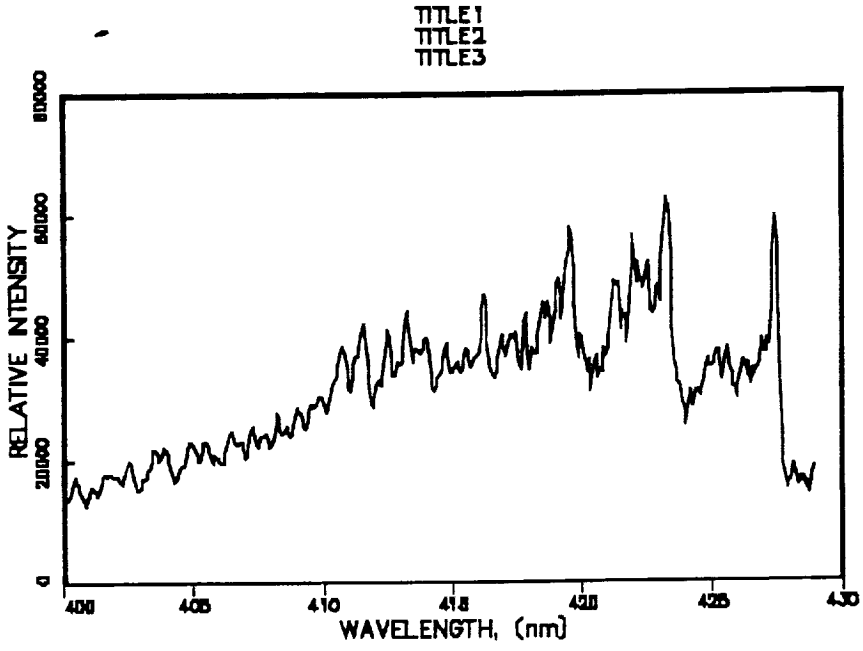

C

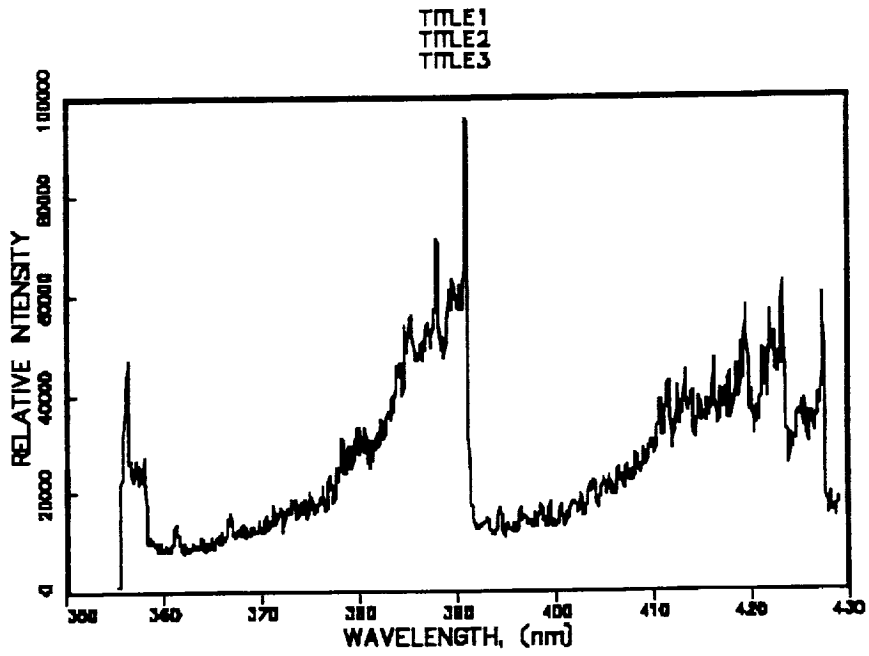
TITLE1
TITLE2
TITLE3
RELATIVE INTENSITY
WAVELENGTH, (nm)

C

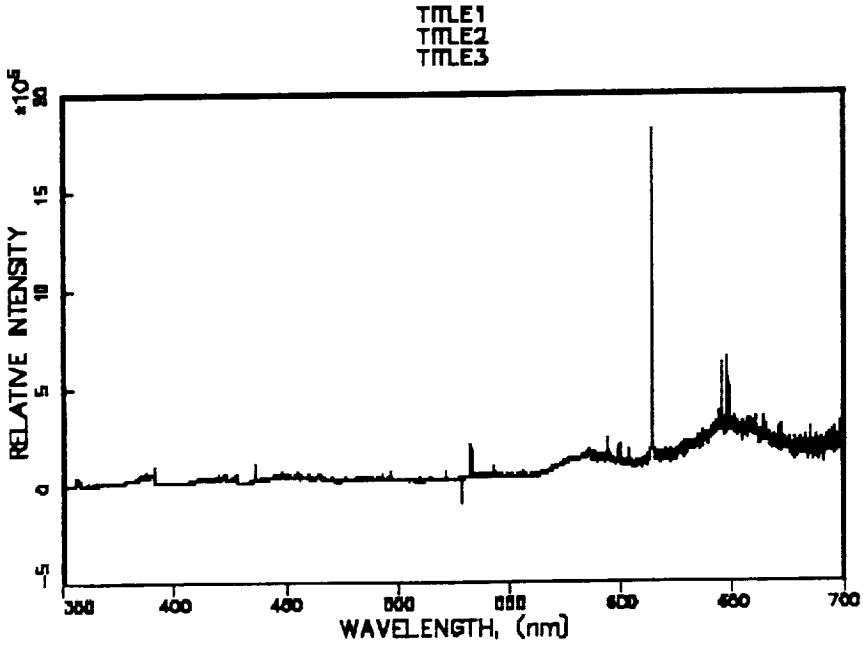
TITLE1
TITLE2
TITLE3
RELATIVE INTENSITY
WAVELENGTH, (nm)

C

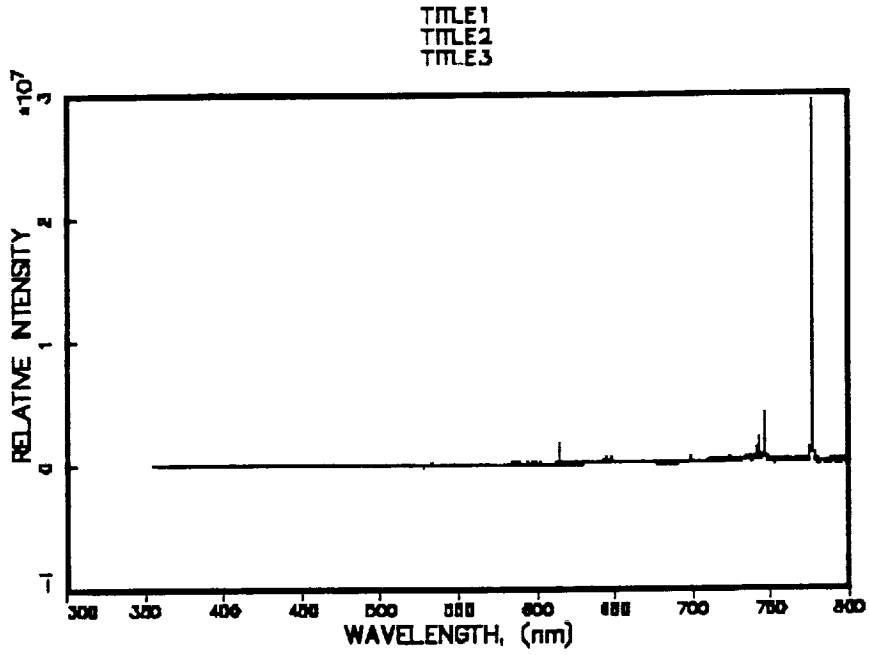

C

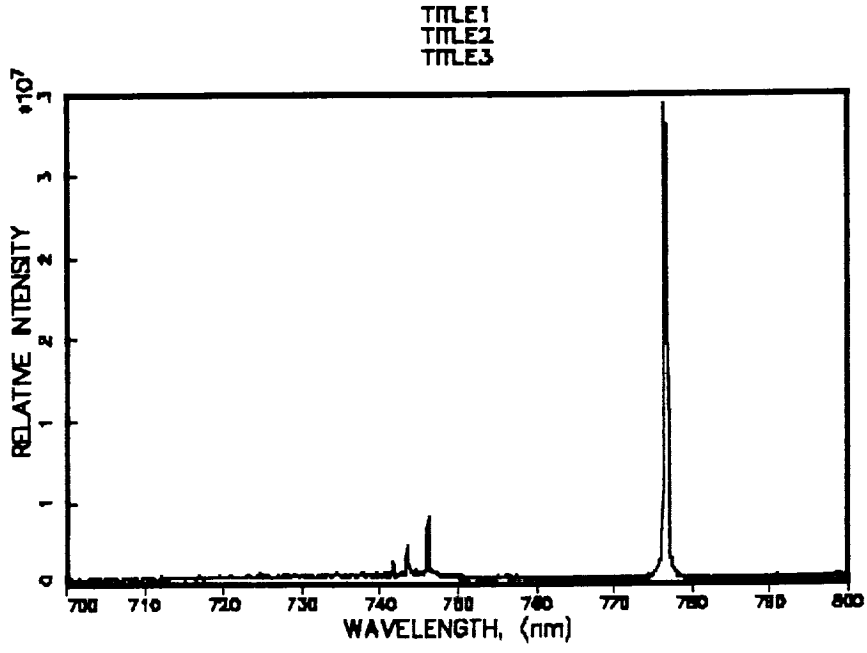

C

Information may be obtained also from the atomic lines.

The air spectra labeled K taken with the flow rate increased to 0.12 lbs/s are shown below.

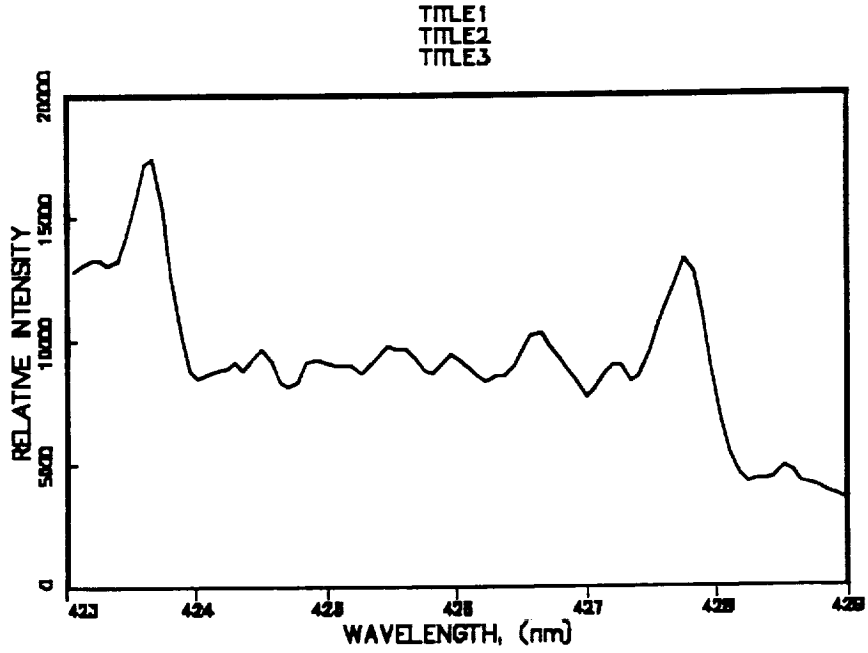

K

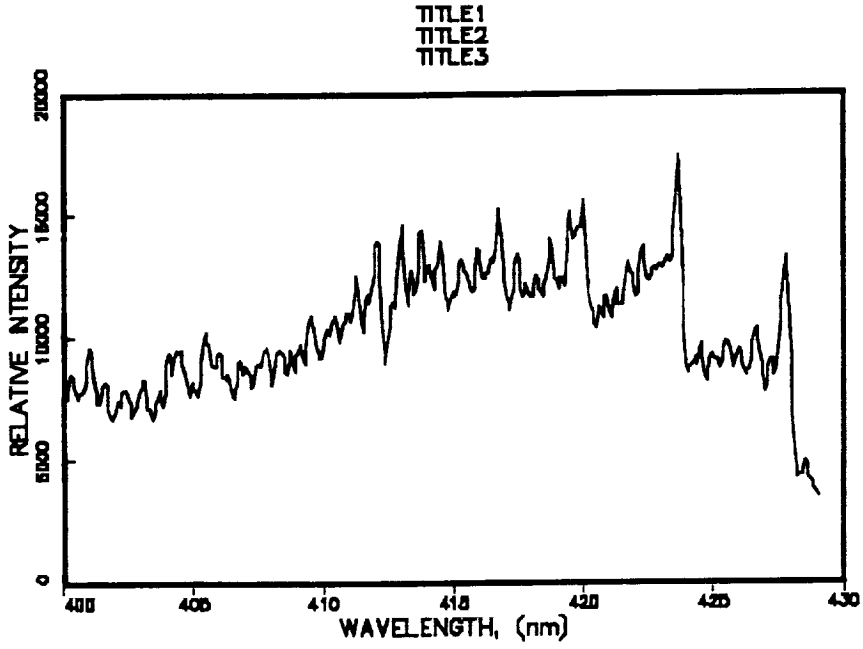

K

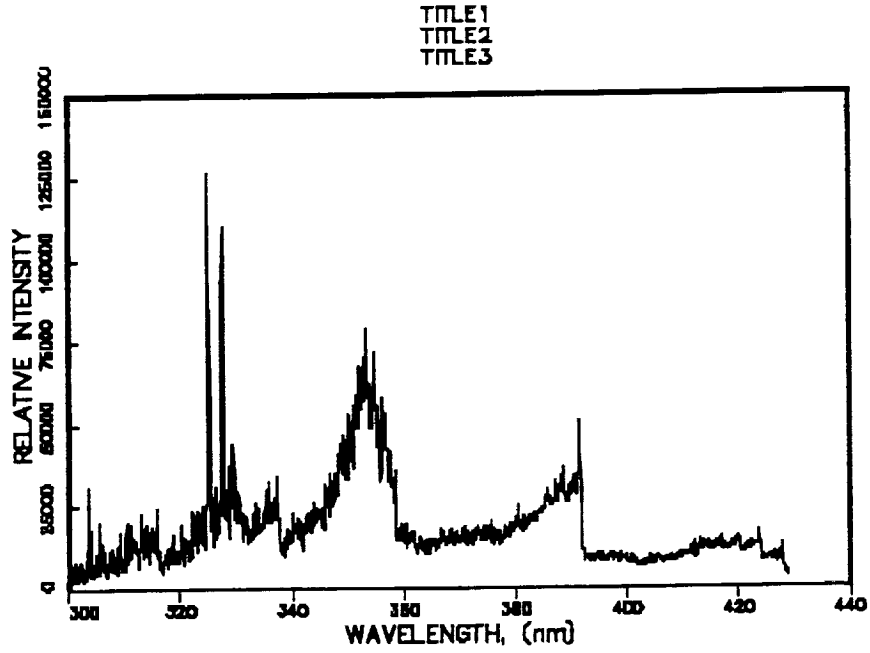
TITLE1
TITLE2
TITLE3
RELATIVE INTENSITY
WAVELENGTH, (nm)

K

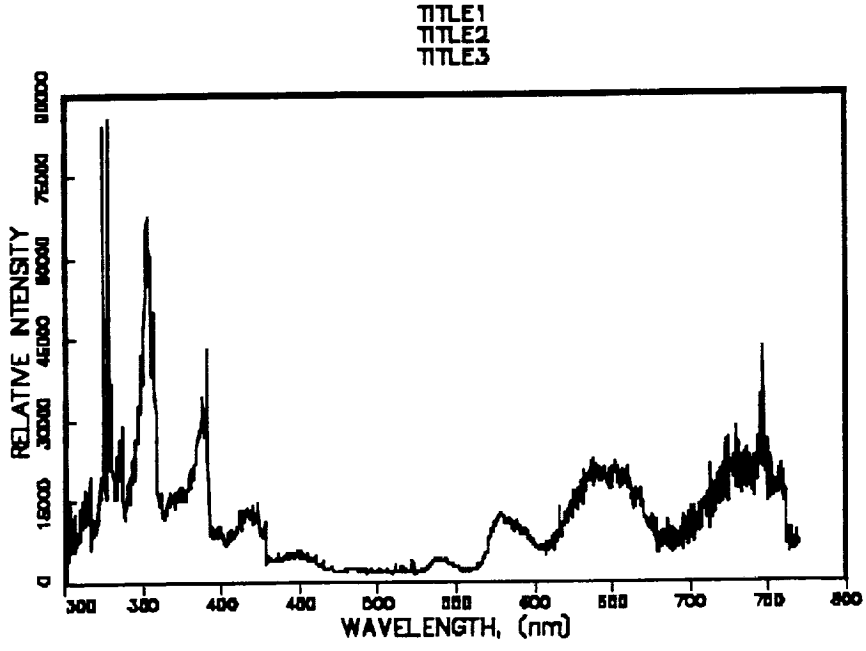
TITLE1
TITLE2
TITLE3
RELATIVE INTENSITY
WAVELENGTH, (nm)

K

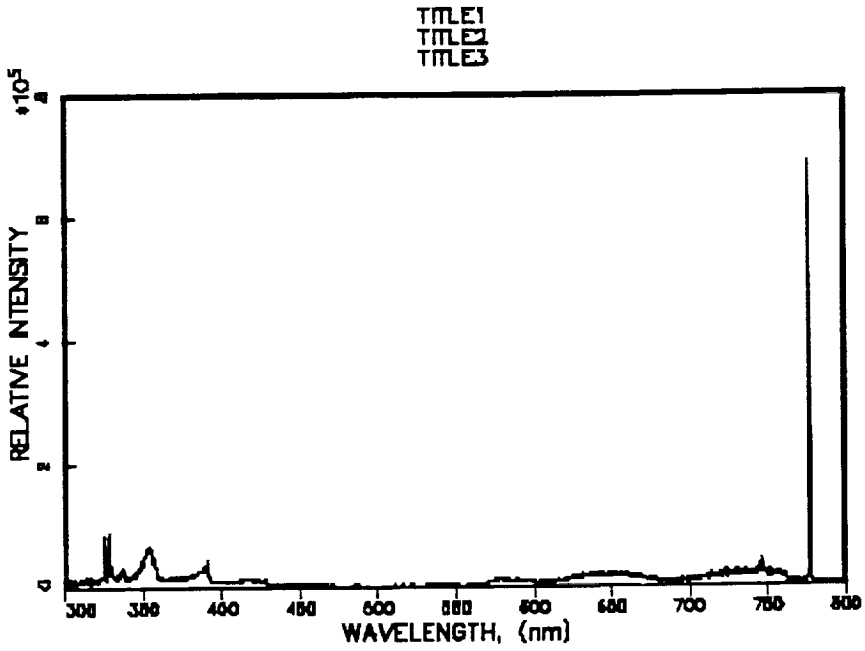

K

APPENDIX D

Included here is the configuration for the mass flow study for which DSMC computational studies have been carried out. Initial cell centers are plotted below and the region boundaries on the following page.

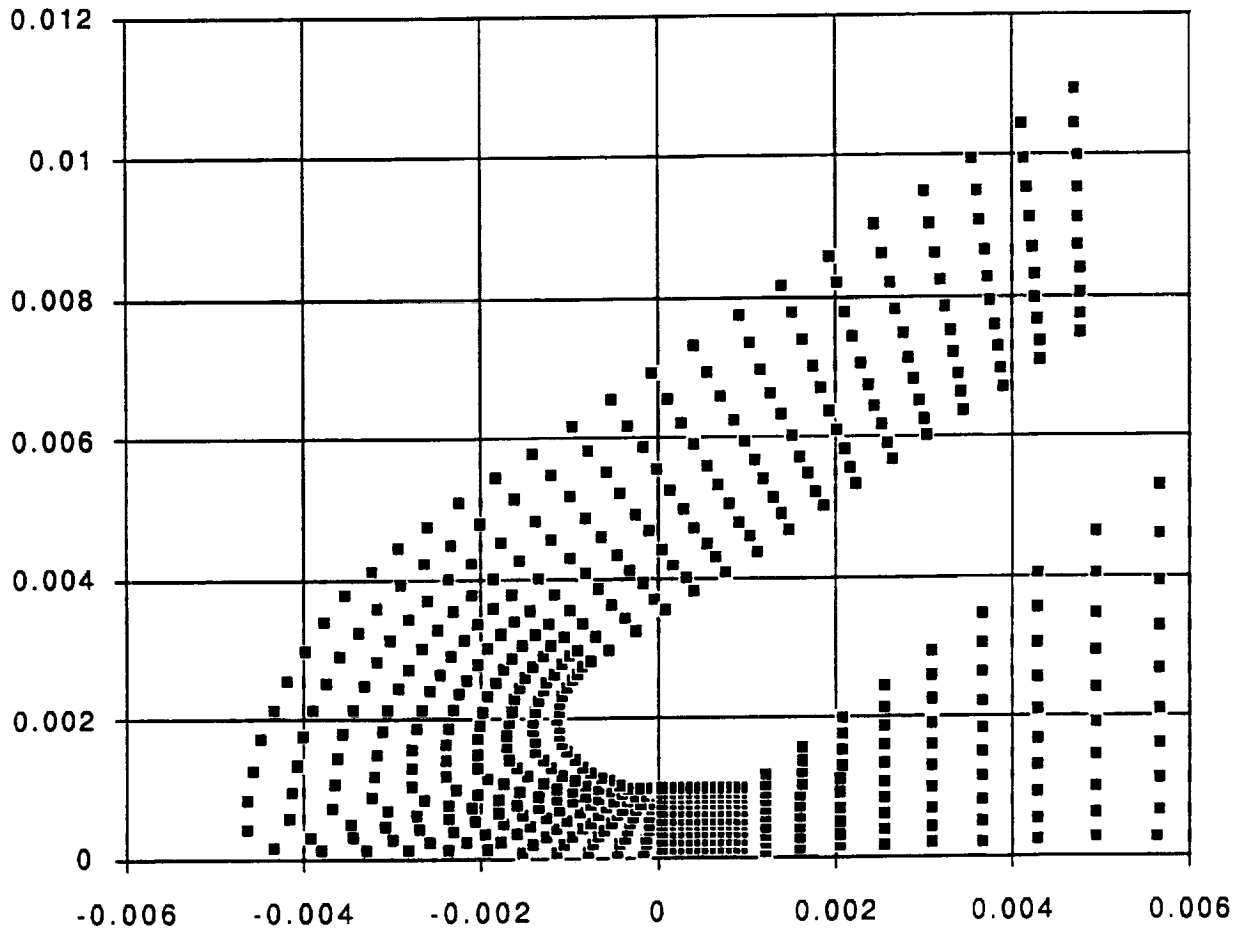

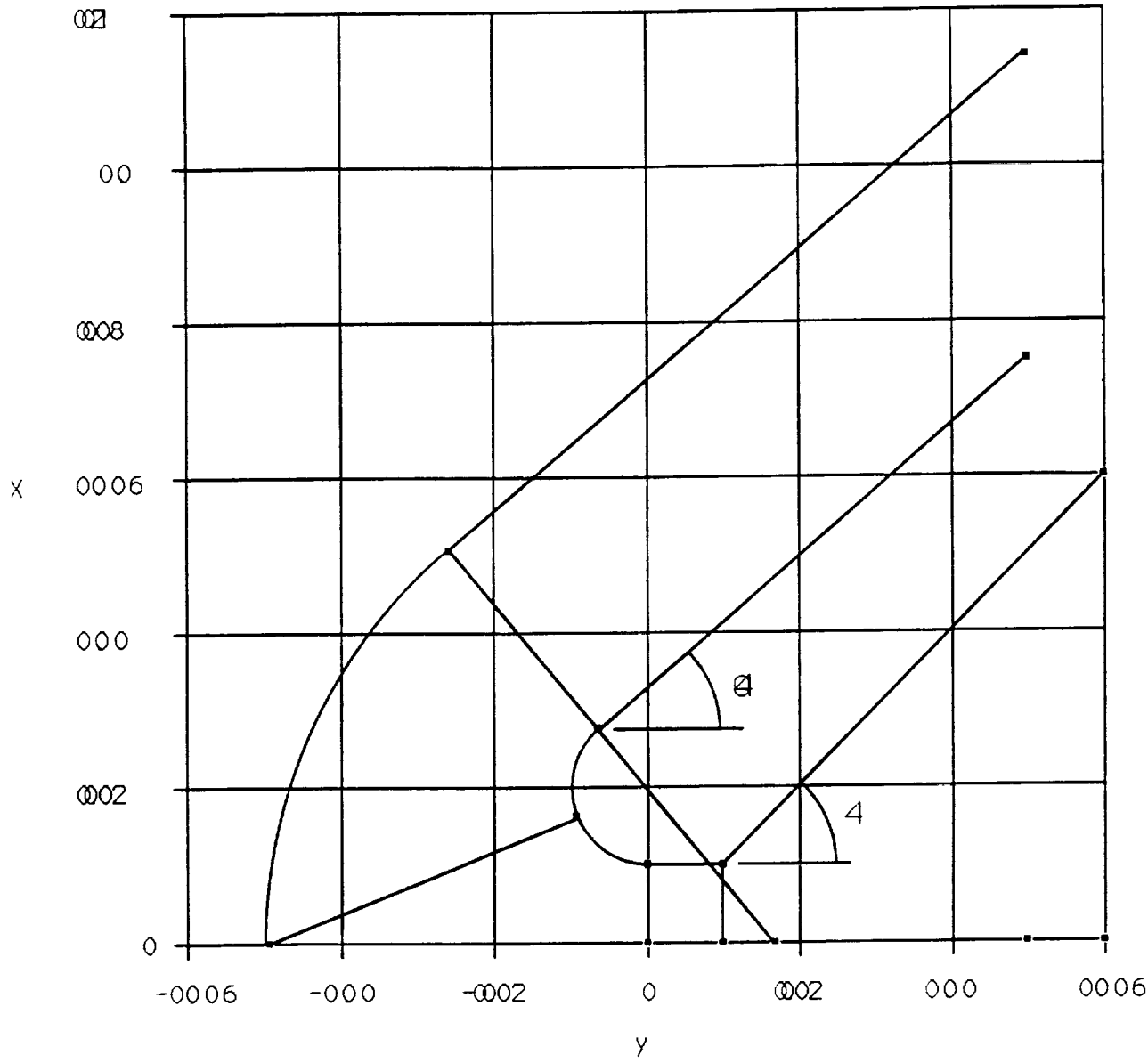
X
y
0
-0006
-000
-0002
0
0002
000
0006
4

APPENDIX E

On the following pages is a draft of the paper on vibrational relaxation to be presented at the AIAA Aerospace Sciences meeting in Reno in January, 1992.

Draft Prepared for AIAA 30th Aerospace Sciences Meeting
January 6-9, 1992, Reno, Nevada

ELECTRON-IMPACT VIBRATIONAL RELAXATION in HIGH-TEMPERATURE NITROGEN

Jong-Hun Lee[1]
BSA Services, Houston, Texas

Abstract

Vibrational relaxation process of N_2 molecules by elecrton-impact is examined for the future planetary entry environments. Multiple-quantum transitions from excited states to higher/lower states are considered for the electronic ground state of the nitrogen molecule $N_2(X^1\Sigma_g^+)$. Vibrational excitation and de-excitation rate coefficients obtained by computational quantum chemistry are incorporated into the "diffusion model" to evaluate the time variations of vibrational number densities of each energy state and total vibrational energy. Results show a non-Boltzmann distribution of number densities at the earlier stage of relaxation, which in turn suppresses the equilibration process. An approximate rate equation and a corresponding relaxation time from the excited states, compatible with the system of flow conservation equations, are derived for the first time. The relaxtion time from the excited states indicates the weak dependency of the vibrational temperature, and is shorter than the previously obtained relaxation time in which only excitation from the ground state was considered. The improved rate equation and the relaxation time, suited for the numerical simulation of the highly ionized planetary entry flowfields, are suggested.

Nomenclature

E_t = total energy
E_v = vibrational energy
E_v^* = equilibrium vibratinal energy at electron temperature, T_e
f = correction factor
h = Planck's constant

[1]Research Scientist. Mailing Address:NASA Johnson Space Center, Houston, TX 77058

J = rotational quantum number
$k_{v,v'}$ = rate coefficients from vibrational state v to v'
K_0 = equivalent diffusivity
M_2 = second moment of vibrational transitions
m = highest vibrational state
m_e = electron mass
n_e = number density of electron
n_M = number density of molecule
n_v = number density of vth excited state
$n_{v'}$ = number density of v'th excited state
p_e = pressure of electron
s = arbitary parameter in rate equation
t = time
T = translational temperature of heavy particle
T_e = electron temperature
T_v = vibrational temperature
v, v' = vibrational quantum number
θ_v = characteristic temperature for vibration
κ = Boltzmann constant
ν = frequency of oscillator
ρ_v = normalized number density of vth state
τ_e = vibrational relaxation time for e-V process

Introduction

Recently, there is an intense worldwide interest on the prosepct of both unmanned and manned exploration of the Moon and the Planet Mars. In order to reduce the weights of vehicles for such future missions, an aerobraking maneuver in the atmosphere is highly desirable. The aerobraking maneuver takes place at the upper atmosphere at very high velocity over extended periods of time. As a result, the flow around such vehicles is expected to be both thermally and chemically in a nonequilibrium state.

While the estimated entry velocity of the aeroassisted orbital transfer vehicle (AOTV) is about or less than 10 km/s, the Lunar-return entry velocity into the Earth's atmosphere is up to about 11 km/s. The proposed Mars-return entry velocity in manned mission is between 11.3 and 14 km/s[1]. Unlike the flow around the AOTV, the flow surrounding the future aeroassited planetary entry vehicle (APEV) will be highly ionized because of higher entry velocities[2].

Due to its light mass, electron-molecule collisions are much more frequent than heavy particle-molecule collisions. Thus electrons are very efficient collisions partners in causing vibrational energy transitions in molecules. In electron-vibration (e-V) energy exchange processes, the Landau-Teller conditions, in

which only the transitions between adjacent levels are allowed, are violated[3]. Therefore, the multiple-level vibrational energy transitions must be considered in the e-V process.

For atmospheric molecules, the low-energy electron-impact vibrational excitation process is usually dominated by resonant mechanism[4]. That is, an incident electron is temporary captured in the neighborhood of a target molecule, thus forming a compound state. This resonance enhances the vibrational excitation cross sections by orders of magnitude. Lee[5] theoretically obtained the vibrational excitation cross sections and rate coefficients for the electronic ground state of the nitrogen molecule $N_2(X^1\Sigma_g^+)$ with the boomerang model of Dube and Herzenberg[6]. Although this method is in principle a semi-empirical one, the obtained cross sections agree reasonably good with the experimental data of Schulz[7].

Lee[5] obtained the analytical solution of the time variation of vibrational energy based on the "diffusion model[8]" at high-temperature regime. Subsequently, an approximate rate equation and a corresponding relaxation time, compatible with the system of flow conservation equations, were developed. Although the obtained relaxation time agrees substantially with experimental result as pointed out by Hansen[9], only the multiple-level excitation from the vibrational ground state is considered in the evaluation. This assumption is valid only for the flow in the vicinity of the shock wave around an vehicle, where most molecules are populated in the vibrational ground state ($v = 0$) at $t = 0$. However, if the flow leaves the shock wave, the contributions of the vibrationally excited states ($v > 0$) become important and the effects of excitation and de-excitation from these $v > 0$ states must be considered. This is especially true for the flow around APEV in which ionization level is much higher than that of AOTV.

The purpose of present paper is to solve numerically the master equation for vibrational transitions from the excited states, and to develop an appropriate rate equation and a relaxation time which approximately represent the rigorous solution of the master equation. The obtained rate equation and the vibrational time for e-V process will be suitable for the numerical simulation of APEV flowfield, since they include the effects of multiple excitation/de-excitation from and to non-ground states.

Vibrational Rate Process

Master Equation for Vibrational Transitions

Assuming that the vibrational oscillators interchange their energies with an electron heat bath having a constant temperature T_e, the rate of change of the

number density n_v without dissociation is given by the master equation

$$\frac{\partial n_v}{\partial t} = \sum_{v'=0}^{m} (k_{v',v} n_{v'} - k_{v,v'} n_v) n_e \tag{1}$$

where n_v is the number density of vth vibrationally excited state, $k_{v,v'}$ the rate coefficient for the transition from state v to v', m the highest vibrational state considered, and n_e the number density of electron. The principle of detailed balancing provides the condition

$$k_{v',v} n_{v'E} = k_{v,v'} n_{vE} \tag{2}$$

where n_{vE} is the equilibrium population in state v. Using the relation (2) and the normalized number density $\rho_v = n_v / n_{vE}$, one obtains the following normalized master equation

$$\frac{1}{n_e} \frac{\partial \rho_v}{\partial t} = \sum_{v'=0}^{m} k_{v,v'} (\rho_{v'} - \rho_v) \tag{3}$$

At the high tempeature regime where the kinetic energy κT_e is larger than the vibrational energy gap, collisional excitation and de-excitation of the vibrational states occur almost in accordance with the classical mechanics[8]. According to the classical analogy, the vibrational energy states are continuously distributed over energy state v, and the summations in Eq. (3) can be replaced by integrations

$$\frac{1}{n_e} \frac{\partial \rho_v}{\partial t} = \int_{v'=0}^{m} k_{v,v'} (\rho_{v'} - \rho_v) dv' \tag{4}$$

If $k_{v,v'}$ in Eq. (4) is assumed to be large only for $|v' - v| < 1$, i.e., the transitions occur mostly between neighboring states, then the the integration limits can be changed from -∞ to ∞

$$\frac{1}{n_e} \frac{\partial \rho_v}{\partial t} = \int_{-\infty}^{\infty} k_{v,v'} (\rho_{v'} - \rho_v) dv' \tag{5}$$

The right-hand side of Eq. (5) is expanded in powers of $\partial^n \rho_v / \partial v^n$, and the terms only to second order are retained , then, one obtains the following diffusion type equation[8,10]:

$$\frac{1}{n_e} \frac{\partial \rho_v}{\partial t} = \frac{\partial}{\partial v} (M \frac{\partial \rho_v}{\partial v}) \tag{6}$$

where

$$M = \frac{1}{2} \int_{-\infty}^{\infty} k_{v,v'} (v' - v)^2 dv' \tag{7}$$

is the second moment of vibrational energy transfer between vth state and v'th state. When $k_{v,v'}$ is given for discrete vibrational states v and v', the moment

M can be determined by summing over the the discrete states

$$M(v) = \frac{1}{2}\sum_{v'}(v'-v)^2 k_{v,v'} \tag{8}$$

The resulting equation (6) is a diffusion equation in the vibrational space v. This equation, together with the requirement that the sum of all n_v's equals the given number density of molecules n_M,

$$n_M = \sum_{v=0}^{m} n_v \simeq \int_0^m n_v dv \tag{9}$$

gives the number density n_v, which is a function of time and energy state v.

Solution of Master Equation

In the following analysis, several assumptions are made. First, the harmonic oscillator model is applied to describe the molecular vibration. Second, the effects of dissociation are neglected. These assumptions are valid rigorously only for the lower vibrational energy states. High vibrational states deviate significantly from the harmonic oscillator assumption due to the anharmonic vibrational potential and the very small unequal energy gaps between the vibrational states[10]. Furthermore, dissociation of molecules depletes the population of upper vibrational states. In gas mixtures with electrons such as the case of planetary entry environments, the electron temperature T_e tends to equilibrate rapidly with the vibrational temperature T_v because of efficient vibrational transitions by electron collisions. When T_v becomes nearly equal to T_e, the electron collisions cause no further change in vibrational populations, even though these temperatures may be far out of equilibrium with the translational temperature of the heavy particle T. After T_e becomes equal to T_v, heavy particle collisions promote T_e and T_v to equilibrate with the heavy particle translational temperature T (Translational-Vibrational energy transfer)[9]. Consequently, the above assumptions are validated at the initial stage of vibrational relaxation, where major transitions are confined to the relatively lower vibrational energy states, in gas mixtures by electron bombardment.

Relaxation from Ground State (Case A)

This is the case the flow immediately behind the shock wave where most molecules are in the ground state at $t = 0$.

Lee[3,5] obtained the analytical solution for Eq. (6) assuming that the spatial variation of the second moment M is small. Then, the normalized number

density ρ_v can be dictated as

$$\rho_v(v,t) = \rho_0[1 - erf\frac{v}{2(K_0 t)^{1/2}}] \tag{10}$$

where $\rho_0 = (n_v/n_{vE})_{v=0}$ is the normalized number density at $v = 0$ and $K_0 = n_e(M)_{v=0}$ is the equivalent diffusivity at $v = 0$, and erf(z) is the error function defined by

$$erf(z) = \frac{2}{\sqrt{\pi}} \int_0^z e^{-\xi^2} d\xi \tag{11}$$

The value of ρ_0 can be approximately assumed to be 1.

The total vibrational energy E_v per unit volume for harmonic oscillators is given by

$$E_v = \sum_{v=0}^{m} vh\nu n_{vE}\rho_v \simeq h\nu \int_0^m v n_{vE}\rho_v dv \tag{12}$$

where h is Planck's constant and ν is the frequency of oscillators. Thus,

$$E_v(t) = A\{\frac{1}{a^2} - \frac{b}{a\sqrt{\pi}} - [1 - erf(\frac{ab}{2})]e^{a^2b^2/4}(\frac{1}{a^2} - \frac{b^2}{2})\} \tag{13}$$

where $A = h\nu n_M(1 - e^{-a})$, $a = \theta_v/T_e$ and $b = 2(K_0 t)^{1/2}$.

The time derivative of $E_v(t)$ can be dictated by

$$\frac{dE_v(t)}{dt} = AK_0\{[1 - erf(\frac{ab}{2})]e^{a^2b^2/4}(1 + \frac{a^2b^2}{2}) - \frac{ab}{\sqrt{\pi}}\} \tag{14}$$

For small t,

$$E_v(t) = A(K_0 t + \cdots) \tag{15}$$

$$\frac{dE_v(t)}{dt} = AK_0 \tag{16}$$

For large t,

$$E_v(t) = A\frac{1}{a^2}(1 - \frac{2}{a\sqrt{\pi}\sqrt{K_0 t}} + \cdots) \tag{17}$$

$$\frac{dE_v(t)}{dt} = \frac{2AK_0}{ab\sqrt{\pi}} \tag{18}$$

Relaxation from Excited State (Case B)

In the flow region away from the shcok wave, the gas has already excited with the vibrational temperature T_v. Therefore, to describe the relaxation process from this excited state, the excitation and de-excitation from/to all levels need

to be considered. Since the second moment of vibrational energy transfer M can not be considered constant in this case, the diffusion equation (6) must be solved numerically. Once the number density of vth excited state $n_v(t)$ is determined numerically, then, $E_v(t)$ and $dE_v(t)/dt$ are calculated.

Since the diffusion equation (6) is the one-dimensional parabolic partial differential equation, the Crank-Nicolson scheme is used to solve the equation numerically.

Rate Equation and Relaxation Time

In the actual numerical simulation, it is quite convenient to use an appropriate rate equation, which is compatible with the system of flow conservation equation, instead of using $E_v(t)$ or $dE_v(t)/dt$ obtained from the diffusion equation. This rate equation corresponds to the source term for vibrational energy equation for a flowing gas. The resulting vibrational energy equation is used in a computaion of nonequilbrium multitemperature flow, along with the conservation equations of mass, momentum, and energy. Therefore, a modified Landau-Teller type of rate equation, which approximate the rigorous solution of Eq. (6), is developed. In order to to derive the rate equation and the relaxation time, an assumption of Boltzmann distribution is made. That is, the vibrational energy levels of molecules are assumed to be populated by a Boltzmann distribution with an unique vibrational temperature T_v.

The rate equation for vibrational relaxation at any given instant may be defined in general as

$$\frac{dE_v(t)}{dt} = \frac{E_v^* - E_v}{\tau_e} f \tag{19}$$

where f is a correction factor and is given by

$$f = \left(\frac{E_v^* - E_v}{E_v^* - E_{v,0}}\right)^{s-1} \tag{20}$$

where superscript and subscript 0 refer to the equilibrium value and the time $t = 0$. Arbitary parameter s in Eq. (20) has a positive value between 1 (Landau-Teller model) and 3.5 (diffusion model).

Neglecting the correction factor in Eq. (19), which is only slightly different from unity, the vibrational relaxation time , τ_e, is given by

$$\tau_e = \frac{E_v^* - E_v}{dE_v(t)/dt} \tag{21}$$

Relaxation from Ground State (Case A)

Since the molecules are all in the ground state at $t = 0$, $E_{v,0}$ in Eq. (20) is zero and therefore, the solution of Eq. (19) is given by

$$E_v(t) = E_v^*\{1 - [1 + (s-1)\frac{t}{\tau_e}]^{\frac{1}{1-s}}\} \tag{22}$$

In this case, τ_e can be approximately given as

$$\tau_e \simeq (\frac{E_v^* - E_v}{dE_v(t)/dt})_{t=0} = \frac{1}{a^2 K_0} = \frac{1}{(\theta_v/T_e)^2 K_0} = \frac{1}{(\theta_v/T_e)^2(1/2)n_e\sum_{v'=0}^{m} k_{0,v'}(v')^2} \tag{23}$$

and the vibrational relaxation time τ_e is independent of the vibrational temperature T_v.

The vibrational relaxation time τ_e in Eq. (23) may be rewritten in the form $p_e\tau_e$ (atm-sec) as

$$p_e\tau_e = \frac{\kappa T_e}{(\frac{\theta_v}{T_e})^2(\frac{1}{2})\sum_{v'=0}^{m} k_{0,v'}(v')^2} \tag{24}$$

Relaxation from Excited State (Case B)

Based on the assumption that the vibrational levels are occupied by a Boltzmann distribution with the vibrational temperature T_v, the vibrational energy $E_{v,0}$ at $t = 0$ is given by

$$E_{v,0} = E_v\,|_{t=0} \equiv E_0 = \frac{n_M h\nu}{e^{\theta_v/T_v} - 1}\,|_{T_{v(t=0)}} \tag{25}$$

The solution of Eq. (19) is

$$E_v = (E_v^* - E_0)\{1 - [1 + (s-1)\frac{t}{\tau_e}]^{\frac{1}{1-s}}\} + E_0 \tag{26}$$

. The numerator of Eq. (21) is defined by

$$E_v^* - E_v = E_v^*(T_e) - E_v(T_v) = n_M h\nu(\frac{1}{e^{\theta_v/T_e} - 1} - \frac{1}{e^{\theta_v/T_v} - 1}) \tag{27}$$

The rate of change of vibrational energy $dE_v(t)/dt$ is established by the excitation and de-excitation rates from/to all levels. For harmonic oscillators

$$\frac{dE_v(t)}{dt} = n_e n_M h\nu \sum_{v=1}^{m}\sum_{v'=0}^{m} \mid v - v' \mid \{(\frac{n_v'}{n_M})k_{v',v} - (\frac{n_v}{n_M})k_{v,v'}\} \tag{28}$$

Thus,

$$\frac{dE_v(t)}{dt} = n_e n_M h\nu(1 - e^{\theta_v/T_v})\sum_{v=1}^{m}\sum_{v'=0}^{m} \mid v - v' \mid \{e^{-v'\theta_v/T_v}k_{v',v} - e^{-v\theta_v/T_v}k_{v,v'}\} \tag{29}$$

In compression flow (heating) case, the number density of v'th energy state is small compared with the one of vth state when $v' > v$, and the excitation rate coefficient $k_{v,v'}$ is much smaller than the de-excitation rate coefficient $k_{v',v}$ when$v \geq 1$. Thus, the sum over v' in Eq. (29) may be chosen as $v' = 0, 1, 2, \cdots, v-1$. That is, the energy gains for all transitions to the state v comes from below, and the energy losses for all transitions from state v goes downward. Then,

$$\frac{dE_v(t)}{dt} = n_e n_M h\nu(1 - e^{\theta_v/T_v}) \sum_{v=1}^{m} \sum_{v'=0}^{v-1} (v - v')(e^{-v'\theta_v/T_v} k_{v',v} - e^{-v\theta_v/T_v} k_{v,v'}) \tag{30}$$

The vibrational relaxation time τ_e is dictated from Eq. (21)

$$\tau_e = \frac{1}{n_e} D \frac{1}{\sum_{v=1}^{m} \sum_{v'=0}^{v-1} (v - v')(e^{-v'\theta_v/T_v} k_{v',v} - e^{-v\theta_v/T_v} k_{v,v'})} \tag{31}$$

where

$$D \equiv \frac{(e^{\theta_v/T_e} - 1)^{-1} - (e^{\theta_v/T_v} - 1)^{-1}}{1 - e^{-\theta_v/T_v}} \tag{32}$$

It must be noted that the relaxation time τ_e in this case is a function of both the vibrational temperature T_v and the electron temperature T_e.

And

$$p_e \tau_e = \kappa T_e D \frac{1}{\sum_{v=1}^{m} \sum_{v'=0}^{v-1} (v - v')(e^{-v'\theta_v/T_v} k_{v',v} - e^{-v\theta_v/T_v} k_{v,v'})} \tag{33}$$

At $T_e, T_v \gg \theta_v$,

$$D \simeq \frac{T_v(T_e - T_v)}{\theta_v^2} \tag{34}$$

Thus, $p_e \tau_e$ can be approximated by

$$p_e \tau_e \simeq \frac{\kappa T_e}{\frac{\theta_v^2}{T_v(T_e - T_v)}} \frac{1}{\sum_{v=1}^{m} \sum_{v'=0}^{v-1} \{(k_{v',v} - k_{v,v'}) + (\theta_v/T_v)(v k_{v,v'} - v' k_{v',v})\}} \tag{35}$$

Results and Discussion

The electronic ground state of the nitrogen molecule $N_2(X^1\Sigma_g^+)$ is considered in the present study, which is the most predominant vibrationally excited molecular species expected in the Earth-return APEV environment. Twelve initial vibrational states ($v = 0 - 12$) are included with 10 quanta change ($\Delta v = v' - v = \pm 10$). Vibrational excitation and de-excitation rate coefficients of N_2, based on computational quantum chemistry[12], are used in the

present calculation. These coefficients obtained by Huo et. al.[12] provide only 5 quanta change ($\Delta v = \pm 5$) because of presumably precipitous dropping of the value for changes of 6 or more vibrational quanta. Hence, these rate coefficients are extrapolated to up to 10 quata change by using the exponential curve fit formula $y = a \cdot exp(-bx)$ in order to give sufficient convergence of the present calculation. The rotaional quantum number $J = 50$ is considered here as only the rate coefficients with this value are available for the present.

Fig. 1 represents the e-V relaxation time in the form $p_e\tau_e$ (atm-sec) for the case A (excitation only from the ground state) given by Eq. (24). As may be seen in Fig. 1, there is virtually no differnce between the result based on Lee's semi-empirical rate coefficients[5] (dotted curve) and the one based on more rigorous coefficients of Huo et. al.[12] (solid curve). These theoretical relaxation times agree substantially with the result based on the experimental values of the cross sections of Schulz[7], except at very low electron temperature ($T_e \simeq 1000\,K$). It must be emphasized that Schulz's experiment was conducted at room temperature, leading to the corresponding rotaional quantum number $J \sim 5$. At low electron temperature, because of the small number density of the electrons with sufficient energy to cause resonant excitation, the contribution of nonresonant excitation (direct excitation) is dominant[5]. In both Lee[5] and Huo et. al.[12] calculations, this nonresonant direct excitation is neglected because of small effects on the excitation mechanism at moderate electron temperatures. Therefore, the experimental result is much more realistic at very low electron temperature.

The e-V relaxation time for case B (excitation/de-excitation from the excited states) given by Eq. (33) is shown in Fig. 2. The relaxation time in this case is a function of both the electron temperature T_e and the vibrational temperature T_v [see Eq. (33)]. The vibrational temperature T_v dictates the initial excited state with a Bolzmann distribution, and the molecules commence to equilibrate from T_v to T_e. As can be seen in Fig. 2, the relaxation times for the case B depend only weakly on the vibrational temperature T_v. The relaxation times become slightly longer with the increse of the vibrational temperature T_v, but the general tendency is exactly the same. The effects of multiple excitation/de-excitation from the excited states contribute to shortening the relaxation times noticeably in the entire temperature range as seen in Fig. 2. As can be deduced from the above-mentioned results, it may be concluded that the e-V relaxation times can be represented by an empirical formula which fits the Schulz's experimental data at very low temperature and the equation (33) with a specific value of T_v (say $T_v = 0.1\,eV$) at moderate and high temperatures. This formula will be a function of the electron temperature T_e only, and applicable to the temperature range of $1000\,K \leq T_e \leq 50000\,K$.

The second moment of vibrational transition rate coefficients $M(v)$ is shown in Fig. 3 for the case where $T_e = 4000\,K$. The $M(v)$ values are good indicator of the overall rate of transitions. $M(v)$ increases rapidly from the ground state

value $M(0)$ and remains nearly constant over the range of $v = 1$ to 12. This trend shows the strong effects of multiple excitation/de-excitation processes in the e-V vibrational transitions. This is also in contrast to the Landau-Teller model in which $M(v)$ increases monotonically with the vibrational level v due to the fact that $k_{v,v+1}$ is proportional to $v + 1$ in the Landau-Teller model[11].

Figure 4 shows the normalized number density ρ_v at selected times. This is a case wherein the molecules, initially in equilibrium at $0.4eV$ with a Boltzmann distribution, is heated suddenly by an electron heat bath having a constant temperature $T_e = 1.0\,eV$. As can be seen in Fig. 4, the population distribution is quite different from a pure Boltzmann distribution in the early stage of relaxation process. Although the populations at $v = 0 - 3$ levels always maintain a Boltzmann distribution (a straight line in the $v - \rho_v$ plot), the populations at $v \geq 4$ considerably deviate from a Boltzmann distribution until at $t = 5.48 \times 10^{-11}$ sec. This underpopulation leads to suppress the equilibration process. Hence, the Boltzmann distribution assumption with unique T_v may be questionable in the relaxation process from the excited states.

The time variation of vibrational energy $E_v(t)$ given by the equation (12) is compared with the solution of rate equation (26) in Fig. 5 for the case of $T_{v(t=0)} = 0.4\,eV$, $T_e = 1.0\,eV$ and for $n_e = 10^{19}\,1/cm^3$. The abscissa in the figure is the time normalized by the relaxation time τ_e [Eq. (31)]. The vibrational energy $E_v(t/\tau_e)$ is normalized by the equilibrium E_v^*. As expected, the solid curve [Eq. (12)] reveals a different feature from the dashed curve [Eq. (26) with $s = 3.5$], due to the suppression phenomenon caused by a non-Boltzmann population distribution. As evident in Fig. 4, the number densities of vibrational levels are underpopulated until $t = 5.48 \times 10^{-11}$ sec, which is corresponding to $t/\tau_e = 5$ in Fig. 5. Because of this underpopulation, the vibrational energy is always smaller than the one predicted by a Boltzmann distribution during the early stage of relaxation. In the case A (relaxation from the ground state), the solution of rate equation (22) with $s = 3.5$ shows the diffusion characteristc, and gives a good agreement with the solution of diffusion equation (13) in the temperature range of $0.1\,eV \leq T_e \leq 2.0\,eV$ [see Ref. (5)]. However, in the case of B (relaxation from the excited states), the agreement is poor because of the profound effectes of underpopulated non-Boltzmann distribution in the early stage of relaxation. The development of more realistic rate equation is required.

At present, effort is being made to obtain an empirical formula for the e-V relaxation time applicable to the temperature range of $1000\,K \leq T_e \leq 50000\,K$. The development of the rate equation, which represents the non-Boltzmann nature in the process of excitation/de-excitation from the excited states, is also underway. These results will be shown in the final paper along with the detailed discussion of the effects of non-Boltzmann distribution on the vibrational equilibration process.

References

[1]Park, C. and Davis, C. B., "Aerothermodynamics of Sprint-Type Manned Mars Mission," AIAA Paper 89-0313, January, 1989, Reno, Nevada.

[2]Park, C., Howe, J. T., Jaffe, R. L., and Candler, G., "Chemical-Kinetic Problems of Future NASA Missions," AIAA Paper 91-0464, January, 1991, Reno, Nevada.

[3]Lee, J. -H., "Basic Governing Equations for the Flight Regimes of Aeroassisted Orbital Transfer Vehicles,' Progress in Astronautics and Aeronautics: Thermal Design of Aeroassisted Orbital Transfer Vehicles, Vol. 96, edited by H. F. Nelson, AIAA, New York, 1985, pp. 3-53.

[4]Schulz, G. J., "A Review of Vibrational Excitation of Molecules by Electon Impact at Low Energies," Principle of Laser Plasmas, edited by G. Bekefi, John Wiley and Sons, New York, 1976, pp. 33-38.

[5]Lee, J. -H., "Electron-Impact Vibrational Excitation Rates in the Flowfield of Aeroassisted Orbital Transfer Vehicles," Progress in Astronautics and Aeronautics: Thermophysical Aspects of Reentry Flows, Vol. 103, edited by J. N. Moss and C. D. Scott, AIAA, New York, 1986, pp.197-224.

[6]Dube, L. and Herzberg, A., "Absolute Cross Sections from the 'Boomerang Model' for Resonant Electron-Molecules Scattering," Physical Review A, Vol. 20, No. 1, July 1979, pp. 1160-1169.

[7]Schulz, G. J., "Vibrational Excitation of Nitrogen by Electron Impact," Physical Review, Vol. 125, January 1962, pp. 229-232.

[8]Keck, J. and Carrier, G., "Diffusion Theory of Nonequilibrium Dissociation and Recombination," Journal of Chemical Physics, Vol. 43, No. 7, July 1965, pp. 2284-2298.

[9]Hansen, C. F., "Vibrational Relaxation in Very High Temperature Nitrogen," AIAA Paper 91-0465, January 1991.

[10]Park, C., "Nonequilibrium Hypersonic Aerothermodynamics," John Wiley & Sons, Inc., New York, 1990.

[11]Sharma, S. P., Huo, W. M., and Park, C., "The Rate Parameters for Coupled Vibration-Dissociation in a Generalized SSH Approximation," AIAA Paper 88-2714, June 1988.

[12]Huo, W. M., McKoy, V., Lima, M. A. P., and Gibson, T. L., "Electron-Nitrogen Molecule Collisions in High-Temperature Nonequilibrium Air," Progress in Astronautics and Aeronautics: Thermophysical Aspects of Reentry Flows, Vol. 103, edited by J. N. Moss and C. D. Scott, AIAA, New York, 1986, pp. 152-196.

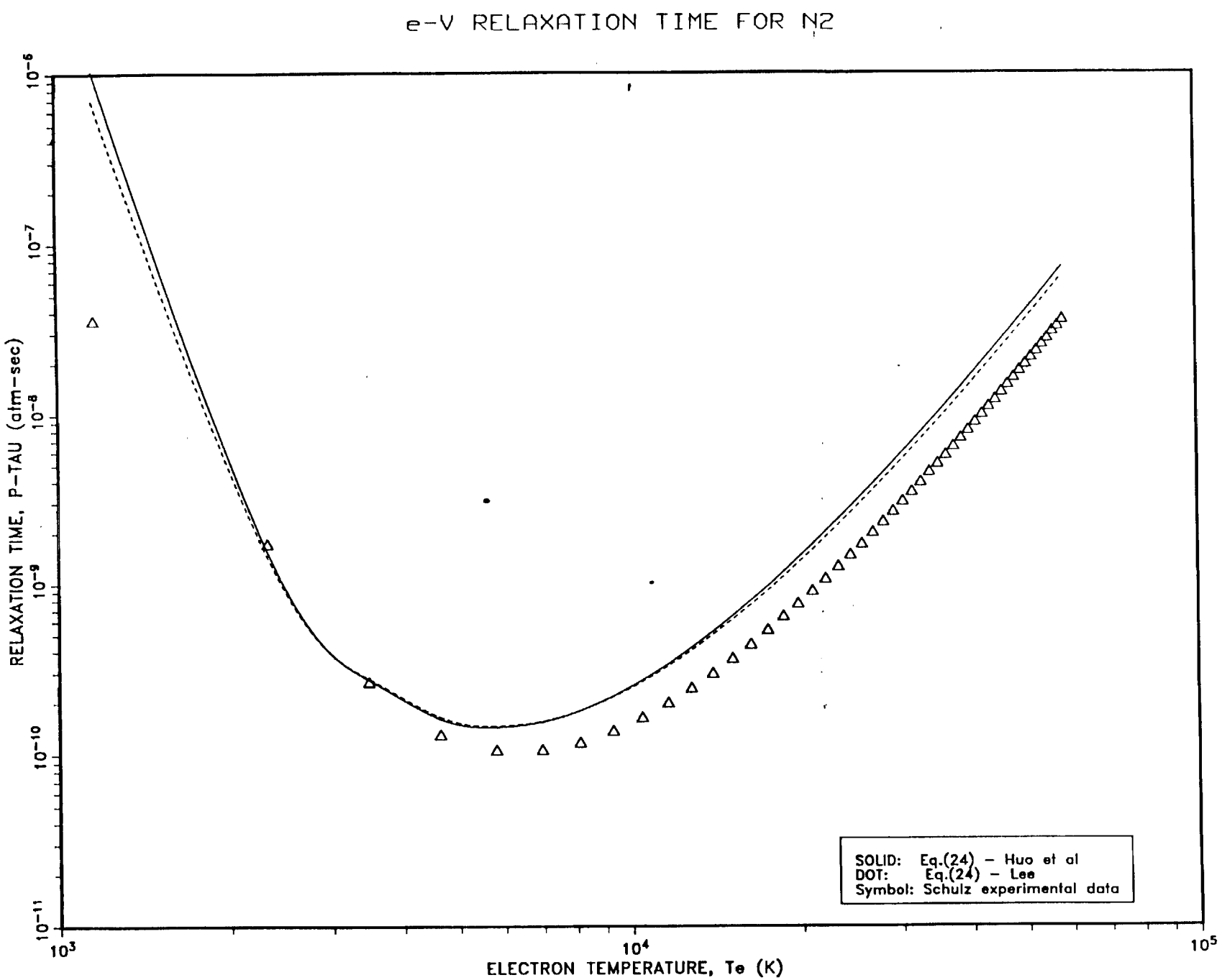

FIG. 1, e-V RELAXATION TIME

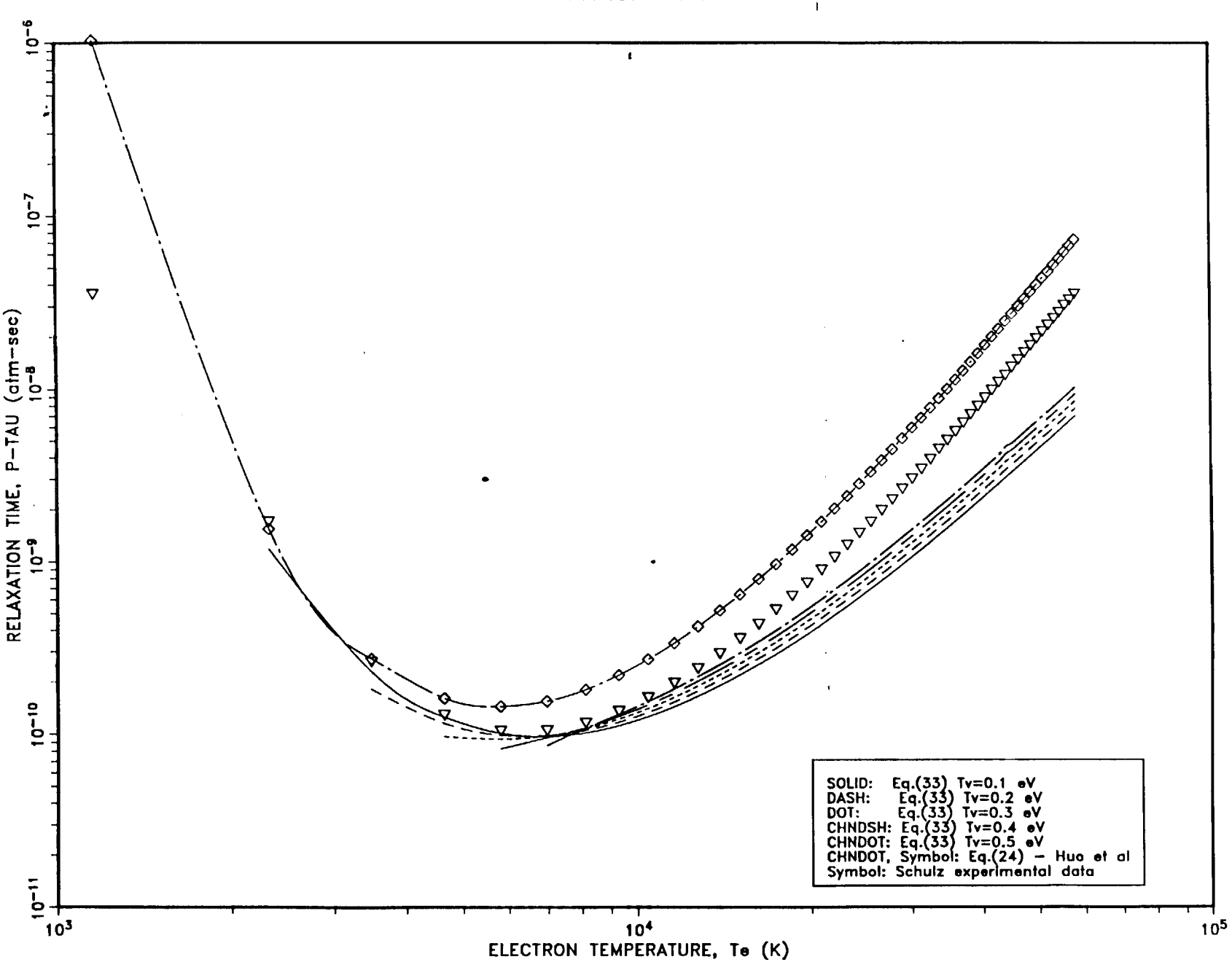

FIG. 2, e–V RELAXATION TIME

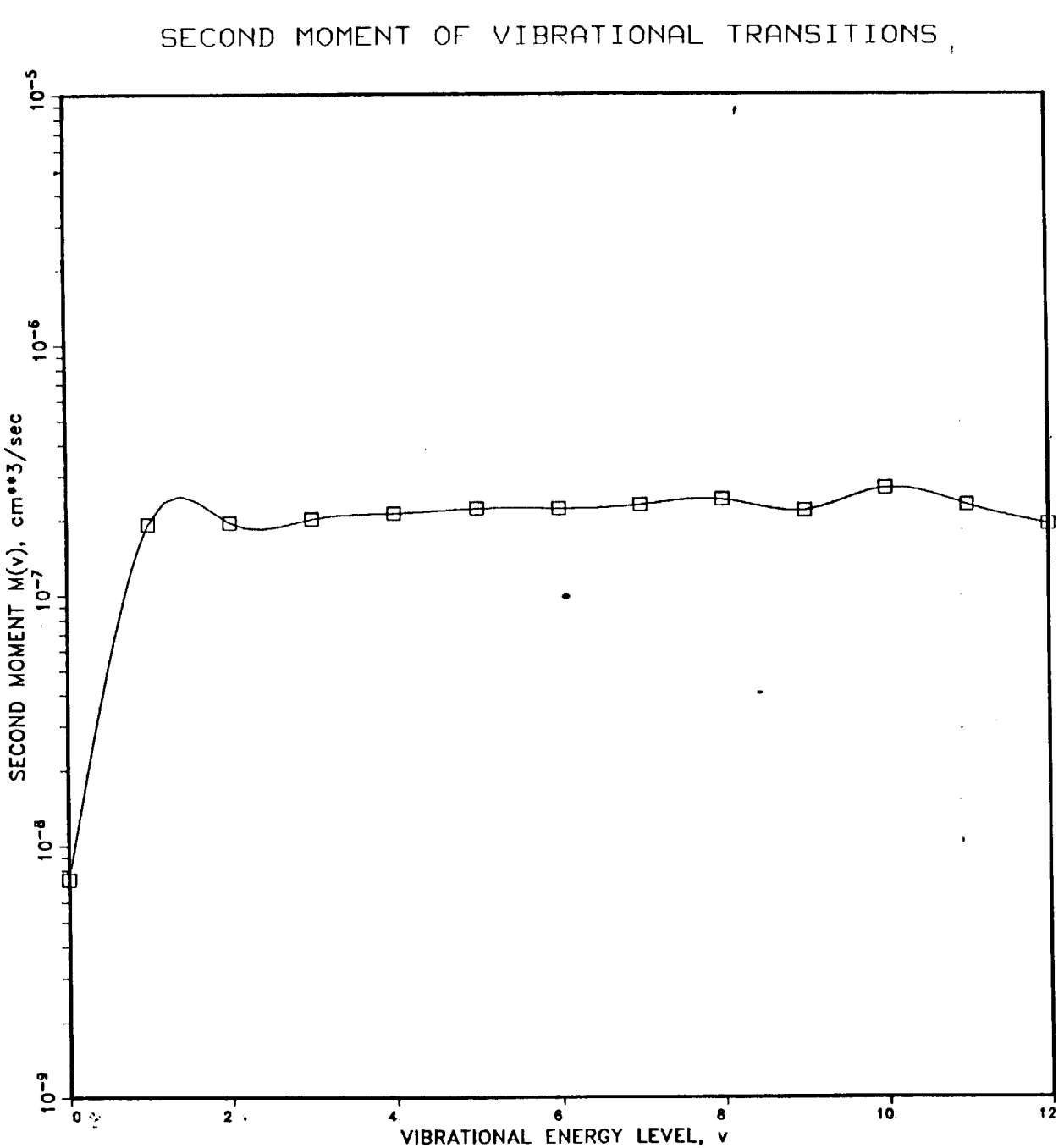

FIG. 3, SECOND MOMENT; Te = 0.4 eV

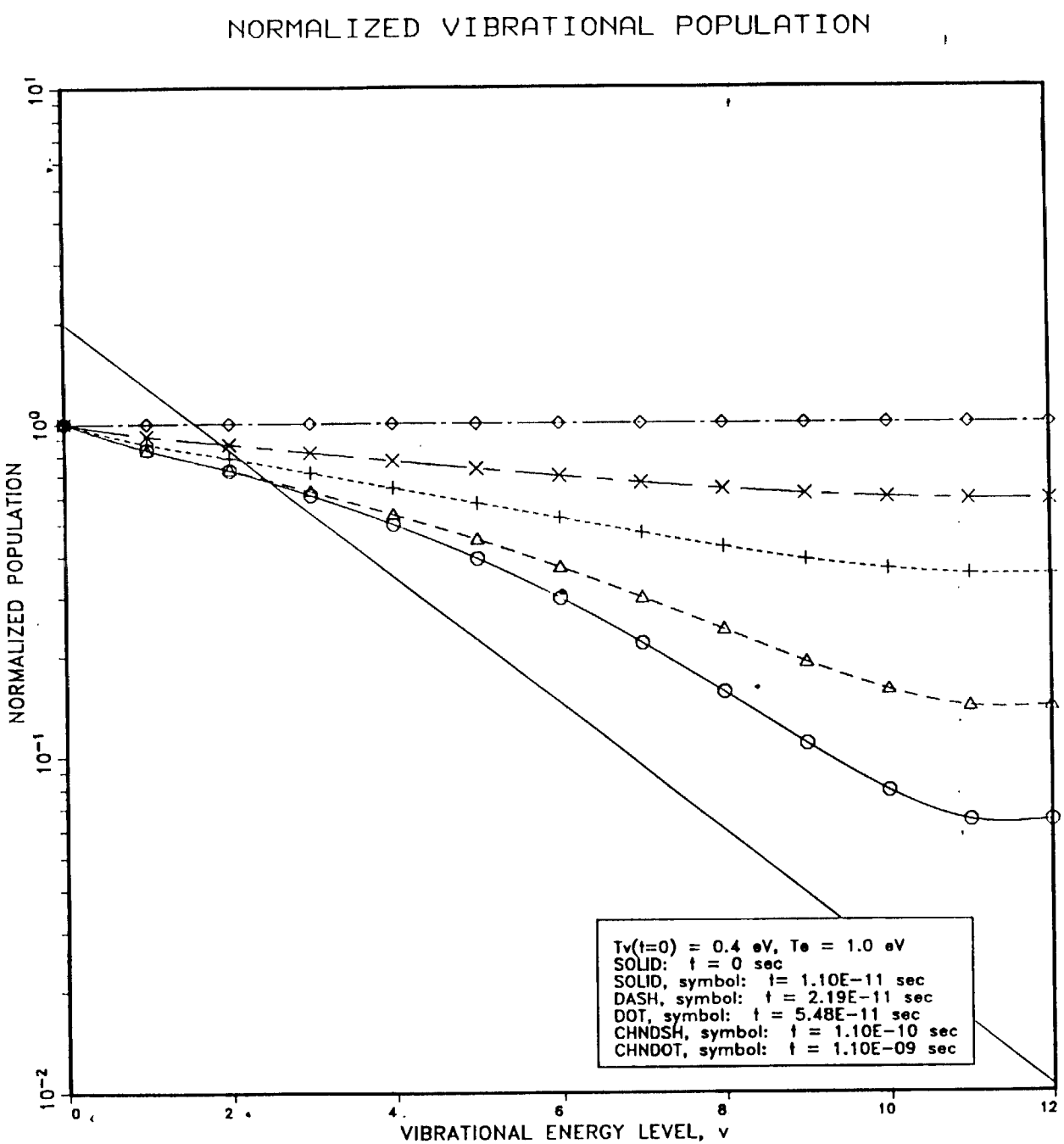

FIG. 4, NORMALIZED VIBRATIONAL POPULATION

SOLUTION OF VIBRATIONAL ENERGY EQUATION

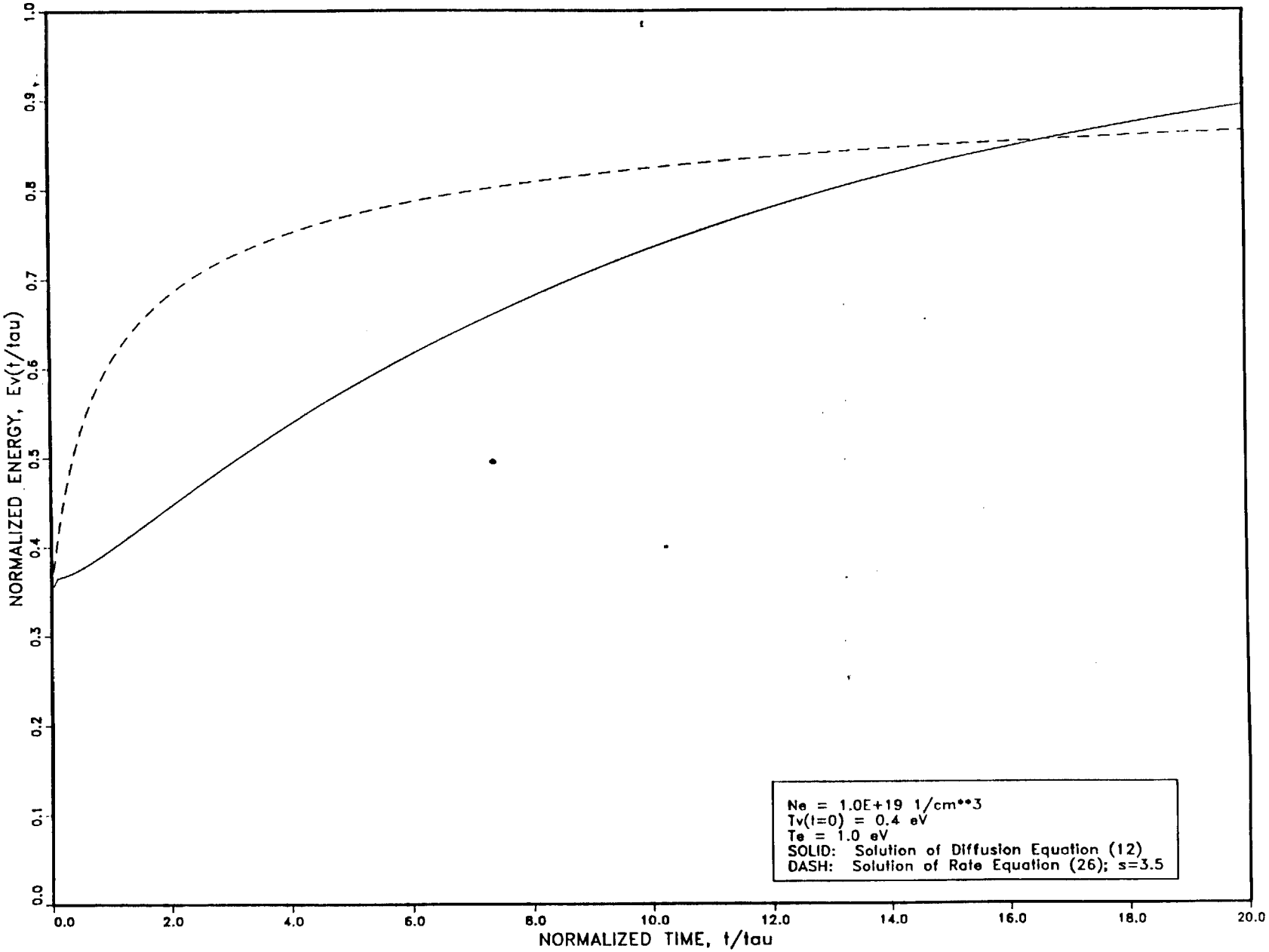

FIG. 5, SOLUTION OF VIBRATIONAL ENERGY EQUATION